ESAIM: M2AN 46 (2012) 81–110
DOI: 10.1051/m2an/2011014

ESAIM: Mathematical Modelling and Numerical Analysis
www.esaim-m2an.org

ON THE STABILITY OF BRAVAIS LATTICES AND THEIR CAUCHY–BORN APPROXIMATIONS *

Thomas Hudson[1] and Christoph Ortner[1]

Abstract. We investigate the stability of Bravais lattices and their Cauchy–Born approximations under periodic perturbations. We formulate a general interaction law and derive its Cauchy–Born continuum limit. We then analyze the atomistic and Cauchy–Born stability regions, that is, the sets of all matrices that describe a stable Bravais lattice in the atomistic and Cauchy–Born models respectively. Motivated by recent results in one dimension on the stability of atomistic/continuum coupling methods, we analyze the relationship between atomistic and Cauchy–Born stability regions, and the convergence of atomistic stability regions as the cell size tends to infinity.

Mathematics Subject Classification. 35Q74, 49K40, 65N25, 70J25, 70C20.

Received November 22, 2010. Revised March 24, 2011.
Published online July 26, 2011.

1. Introduction

Over the past decade there has been increasing interest in the applied analysis literature on connecting atomistic and continuum models of crystalline solids; see, *e.g.*, [1,2,4,7,8,20,21]. These results focus primarily on the rigorous derivation of continuum limits from discrete models, using, *e.g.*, Γ-convergence techniques [1,4,20] or an inverse function theorem combined with elliptic regularity results and asymptotic expansions [7].

In the present paper, we investigate the stability of Bravais lattices when described by an atomistic model and by its corresponding Cauchy–Born approximation. We are particularly interested in the relationship between stability in the atomistic model and continuum model, and in the convergence of atomistic stability constants (and stability regions) as the number of atoms in a periodic cell tends to infinity. The present work provides a crucial technical ingredient for our ongoing analysis of the Cauchy–Born approximation, and serves as a preliminary step and motivation for a similar stability analysis of atomistic/continuum coupling methods as in [5]. In the following paragraphs we provide a more detailed motivation for this work.

We remark that the Cauchy–Born approximation provides an accurate model for crystal elasticity only at zero (or very low) temperature. All our subsequent discussions assume zero temperature statics.

Keywords and phrases. Bravais lattice, Cauchy–Born model, stability.

* *This work was supported by an undergraduate vacation bursary of the Oxford Centre for Nonlinear PDE (funded by EPSRC), and by the EPSRC grant "Analysis of atomistic/continuum coupling methods".*

[1] Mathematical Institute, Oxford, OX1 3LB, UK. ortner@maths.ox.ac.uk; thomas.hudson@maths.ox.ac.uk

1.1. Motivation

Since Γ-convergence techniques tend to "smear out" realistic interaction potentials, and in the process "destroy" information contained in the atomistic model, the inverse function theorem approach [7] seems to be better suited to treat realistic atomistic models (without modifying the potentials). Moreover, it has the advantage that it provides explicit convergence rates. On the downside, it requires far more detailed information about the atomistic model and the regularity of solutions. A possible approach to make the connection between atomistic and continuum models rigorous is the following:

1. Derive the Cauchy–Born continuum limit (see [2] and Sect. 2 in the present paper). Compute a solution of the Cauchy–Born equations, or assume the existence of such a solution y_c, with sufficiently high regularity (at least $C^{1,\alpha}$).
2. Use consistency of the atomistic and Cauchy–Born models to show that y_c approximately satisfies the atomistic equilibrium equations.
3. Prove stability of the atomistic model, linearized at y_c, and an inverse function theorem to prove the existence of an equilibrium y_a in a small neighbourhood of y_c.

Variants of this proof outline can be found, *e.g.*, in [7,18,19]. Possibly the most important step is to justify the stability of the atomistic model, linearized at y_c. The fundamental question, which arises, is the following: if y_c is a *stable equilibrium* of the Cauchy–Born model, does this imply that the atomistic model, linearized at y_c is also stable? If the answer to this question is positive then this implies (up to some technical assumptions) that *any smooth and stable equilibrium of the Cauchy–Born model approximates a stable equilibrium of the atomistic model.*

In the present paper we investigate this question for the case of homogeneous deformations (*i.e.*, Bravais lattices), which can be considered a simplified case, but also arises in the above stability analysis through blow-up arguments.

Apart from posing this as an interesting analytical problem, we note that this question necessarily arises whenever the Cauchy–Born model is used to simulate a crystalline solid; see, *e.g.*, [23]. The same question has also arisen in the numerical analysis literature on atomistic/continuum coupling methods [5,6]. If an atomistic/continuum coupling method is used to predict a bifurcation point (*e.g.*, the onset of motion or formation of a dislocation) then it must be guaranteed that the stability regions of the atomistic/continuum method and of the full atomistic model coincide up to a controllable error, at least in a region of interest.

In addition to understanding the connection between atomistic and Cauchy–Born stability, it is useful to have information about the convergence rate of the atomistic stability constant as the number of atoms in a periodic cell tends to infinity. This problem arises in various scenarios. (i) It tells us how large an atomistic system needs to be to justify working with the limiting stability condition. (ii) If the atomistic and Cauchy–Born stability regions do not coincide then one ought to monitor the atomistic stability condition during simulations with a Cauchy–Born or coupled atomistic/continuum model. These can be computed on finite periodic cells, and convergence rates are required to justify the choice of grids. (iii) Finally, if we reverse the role of y_a and y_c in the argument 1.–3. above, that is, we assume the existence of a stable atomistic equilibrium, then we need to test whether y_a is also stable in the continuum model. We will see that this is always true in the limit as the number of atoms tends to infinity, and hence require convergence rates for finite cells in order to quantify this.

1.2. Outline

The stability of Bravais lattices under different interaction potentials has been investigated for many decades, primarily by physicists and materials scientists; see, *e.g.*, [3,12,22] for classical treatments of the subject. A general technique that is particularly useful for computational experiments is to rephrase the problem in reciprocal space using a (semi-)discrete Fourier transform (cf. Sect. 1.4.3).

This transform leads to useful characterisations of the atomistic and Cauchy–Born stability constants, $\Lambda_a(\mathsf{B})$ and $\Lambda_c(\mathsf{B})$ (the smallest H^1-eigenvalues of the Hessian operators; see Sect. 3), which are parameterised by

matrices $\mathsf{B} \in \mathbb{R}^{d\times d}$ describing the orientation of the Bravais lattice. The lattice is stable in the atomistic model if $\Lambda_{\rm a}(\mathsf{B}) > 0$ and in the continuum model if $\Lambda_{\rm c}(\mathsf{B}) > 0$.

Our first result is that $\Lambda_{\rm c}(\mathsf{B}) \le \Lambda_{\rm a}(\mathsf{B})$ holds for all matrices $\mathsf{B} \in \mathbb{R}^{d\times d}$, that is, the atomistic stability region is always contained in the continuum stability region. This is a well-known result (see [22], p. 89 for a formal argument), however, we give a simpler and, we believe, more illuminating proof that does not require reciprocal space techniques (Sect. 3.1).

The proof we present, as well as Wallace's argument clearly indicate that there is no reason to expect that the two stability regions should coincide. Therefore, as discussed in previous paragraphs, it is of interest to investigate the convergence rate of $\Lambda_{\rm a}^N(\mathsf{B}) \to \Lambda_{\rm a}(\mathsf{B})$, where $\Lambda_{\rm a}^N(\mathsf{B})$ denotes the stability constant for a $2N \times \cdots \times 2N$ periodic cell. We show that this rate is $O(N^{-1})$ in the worst case (Sect. 4). We then show how to construct alternative grids in reciprocal space, which contain $O(M^d)$ grid points, and which lead to an $O(M^{-2})$ convergence rate (Sect. 4.7).

Finally, in Section 5, we discuss a simple analytical example as well as several numerical examples where the atomistic and Cauchy–Born stability regions do coincide. We are currently unable to justify these numerical results either rigorously or heuristically, but we believe they provide motivation for further study of this interesting issue. We also give a physically relevant counterexample.

1.3. **The atomistic model in a periodic domain**

Let $d \ge 1$, $N \in \mathbb{N}$ and $\varepsilon = 1/(2N)$ be fixed throughout. We define the discrete periodic domain

$$\Omega_N = \varepsilon\{-N+1, -N+2, \dots, N\}^d = \left\{-\tfrac{1}{2}+\varepsilon, -\tfrac{1}{2}+2\varepsilon, \dots, \tfrac{1}{2}\right\}^d,$$

and the set of periodic displacements

$$\mathscr{U}_N = \left\{u : \varepsilon\mathbb{Z}^d \to \mathbb{R}^d : u(x+e_j) = u(x) \text{ for } x \in \varepsilon\mathbb{Z}^d, j = 1, \dots, d\right\}.$$

The homogeneous deformation with deformation gradient $\mathsf{B} \in \mathbb{R}^{d\times d}$, $\det \mathsf{B} > 0$, is defined as

$$y_{\mathsf{B}}(x) = \mathsf{B}x \qquad \text{for } x \in \varepsilon\mathbb{Z}^d.$$

A homogeneous deformation is also called a *Bravais lattice*. The set of periodic deformations with underlying macroscopic strain B is

$$\mathscr{Y}_N = y_{\mathsf{B}} + \mathscr{U}_N = \left\{y : \varepsilon\mathbb{Z}^d \to \mathbb{R}^d \text{ s.t. } y - y_{\mathsf{B}} \in \mathscr{U}_N\right\}.$$

For a discrete function $v : \varepsilon\mathbb{Z}^d \to \mathbb{R}^d$, for $x \in \varepsilon\mathbb{Z}^d$ and for $\rho \in \mathbb{Z}^d$, we define the forward difference operator

$$D_\rho v(x) = \frac{v(x+\varepsilon\rho) - v(x)}{\varepsilon}.$$

Let $\mathscr{R} \subset \mathbb{Z}^d \setminus \{0\}$ be a finite set, which we call the *interaction range*, and let $D_{\mathscr{R}}$ denote the family of all differences D_ρ, $\rho \in \mathscr{R}$, that is

$$D_{\mathscr{R}} v(x) = \big(D_\rho v(x); \rho \in \mathscr{R}\big).$$

Let $V : (\mathbb{R}^d)^{\mathscr{R}} \to \mathbb{R} \cup \{+\infty\}$ be the *interaction potential*. We then define the atomistic energy of a deformation $y \in \mathscr{Y}_N$ as

$$E_N^{\rm a}(y) = \varepsilon^d \sum_{x\in\Omega_N} V(D_{\mathscr{R}} y(x)).$$

1.3.1. *Differentiability of $E_N^{\rm a}$*

We assume throughout that $V \in \mathrm{C}^3(D_V)$ where D_V is the *domain* of V,

$$D_V = \big\{(a_\rho)_{\rho\in\mathscr{R}} \in (\mathbb{R}^d)^{\mathscr{R}} : a_\rho \neq 0 \text{ for all } \rho \in \mathscr{R}, \text{ and } a_\rho \neq a_{\rho'} \text{ for all } \rho, \rho' \in \mathscr{R}, \rho \neq \rho'\big\}.$$

Thus, D_V denotes the set of all configurations where the positions of any two atoms are distinct. Under this assumption, it follows that $E_N^{\rm a}$ has three continuous derivatives at any deformation y such that $y(x) \neq y(x')$ for all $x, x' \in \varepsilon\mathbb{Z}^d$.

To obtain uniform bounds on the derivatives of $E_N^{\rm a}$ it is convenient to define compact subsets of the domain of V,

$$D_V^\delta = \big\{(a_\rho)_{\rho\in\mathscr{R}} : \delta \leq |a_\rho| \leq \delta^{-1} \text{ for all } \rho \in \mathscr{R}, \text{ and } \delta \leq |a_\rho - a_{\rho'}| \text{ for all } \rho, \rho' \in \mathscr{R}, \rho \neq \rho'\big\}.$$

Since $V \in \mathrm{C}^3(D_V)$ it follows that all partial derivatives of V are bounded above in D_V^δ, that is, for $k = 0, 1, 2, 3$ we define

$$M_k^\delta := \sup_{(a_\rho)_{\rho\in\mathscr{R}} \in D_V^\delta} \max_{\substack{\alpha\in\mathscr{R}^k \\ |\alpha|_1 = k}} |\partial_\alpha V(a_\rho; \rho \in \mathscr{R})|,$$

where we used multiindex notation for partial derivatives and $|\cdot|$ denotes the ℓ^2-norm of the components of a tensor of any order.

1.3.2. *Symmetry of V*

We conclude this section with a discussion of the symmetry properties of V. Let I_d denote the identity map on $\mathbb{R}^d$. We assume throughout that $\mathscr{R}$ is invariant under the transformation $-\mathsf{I}_d$, that is if $\rho \in \mathscr{R}$ then $-\rho \in \mathscr{R}$. Moreover, we assume that V has the symmetry property

$$V(-a_\rho; \rho \in \mathscr{R}) = V(a_{-\rho}; \rho \in \mathscr{R}) = V(a_\rho; \rho \in \mathscr{R}) \text{ for all } (a_\rho)_{\rho\in\mathscr{R}} \in (\mathbb{R}^d)^{\mathscr{R}}. \tag{1.1}$$

An immediate consequence of this assumption is the following symmetry of the first and second partial derivatives

$$\begin{aligned} \partial_\rho V(D_{\mathscr{R}} y_{\mathsf{F}}) &= -\partial_{-\rho} V(-D_{-\mathscr{R}} y_{\mathsf{F}}) \qquad \forall \rho \in \mathscr{R} \quad \forall \mathsf{F} \in \mathbb{R}^{d\times d}, \qquad \det \mathsf{F} > 0, \\ \partial_\rho \partial_\sigma V(D_{\mathscr{R}} y_{\mathsf{F}}) &= \partial_{-\sigma} \partial_{-\rho} V(D_{\mathscr{R}} y_{\mathsf{F}}) \qquad \forall \rho, \sigma \in \mathscr{R} \quad \forall \mathsf{F} \in \mathbb{R}^{d\times d}, \qquad \det \mathsf{F} > 0. \end{aligned} \tag{1.2}$$

Remark 1.1.

1. Choosing the reference domain to be symmetric about the origin will simplify some of our subsequent analysis involving the Fourier transform. The resulting restriction, that the number of atoms in each coordinate direction is even, can be lifted with some additional work. Moreover, we note that the direct proof of Theorem 3.1, which does not use Fourier transform techniques, can be repeated for general N without changes. The trigonometric interpolant (which we define next) used in this proof can be replaced by any other reasonable choice, *e.g.*, a Q1 interpolant on the canonical finite element mesh induced by the grid $\varepsilon\mathbb{Z}^d$.
2. The scaling for the domain, the energy, and the finite differences were chosen to yield a natural Cauchy–Born continuum limit, which we discuss in Section 2. While other scalings are also natural, and have their advantages, we wanted to particularly stress the connection to continuum elasticity.
3. We emphasize that the set $\mathscr{R}$ describes the interaction range in the reference configuration, which is usually not suitable for atomistic models. However, since we can choose $\mathscr{R}$ arbitrarily large (but finite) and since we do not consider significant rearrangements of atoms this is no restriction of generality.

We expect that one can accommodate an infinite interaction range with sufficiently fast decay in our analysis, however, for the sake of simplicity we decided to work with a finite interaction range only.

4. Realistic interaction potentials have the property that any permutation of the nuclei does not change the potential, that is, for any permutation π of $\mathscr{R}$ we have

$$V(a_\rho; \rho \in \mathscr{R}) = V(a_{\pi\rho}; \rho \in \mathscr{R}).$$

Moreover, a reflection of the configuration about the origin cannot change the potential either, that is,

$$V(a_\rho; \rho \in \mathscr{R}) = V(-a_\rho; \rho \in \mathscr{R}).$$

Combining these two properties we obtain the point symmetry property (1.1).

1.4. **Fourier transforms and reciprocal domains**

In this section we collect some notation and standard results on the Fourier transforms of discrete and continuous functions.

The domain for continuous functions, corresponding to the discrete domain Ω_N, is $\Omega = (-\frac{1}{2}, \frac{1}{2}]^d$, and the spaces of periodic functions we will use are

$$\mathrm{C}^{k,\alpha}_{\mathrm{per}}(\Omega) = \big\{v \in \mathrm{C}^{k,\alpha}(\mathbb{R}^d) : v \text{ is } \Omega\text{-periodic}\big\}, \quad \text{for } k \geq 0, \alpha \in [0,1], \quad \text{and}$$
$$\mathrm{H}^1_{\mathrm{per}}(\Omega) = \big\{v \in \mathrm{H}^1_{\mathrm{loc}}(\mathbb{R}^d) : v \text{ is } \Omega\text{-periodic}\big\},$$

with associated norms $\|\cdot\|_{\mathrm{C}^{k,\alpha}}$ and $\|\cdot\|_{\mathrm{H}^1}$. We remark that all spaces $\mathrm{C}^{k,\alpha}_{\mathrm{per}}(\Omega)$, $k \geq 1$, $\alpha \in [0,1]$, are dense in $\mathrm{H}^1_{\mathrm{per}}(\Omega)$. We will also frequently use the L^∞-norm $\|\cdot\|_{\mathrm{L}^\infty}$ and the L^2-norm $\|\cdot\|_{\mathrm{L}^2}$.

For future reference we also define ∇v to be the Jacobi matrix of a differentiable function v, and $\nabla_r v = (\nabla v) r$ the directional derivative.

1.4.1. *Discrete functions*

The discrete *reciprocal domain* (with respect to the scaled *physical domain* Ω_N) is

$$\widehat{\Omega}_N = \big\{(-N+1)\pi, (-N+2)\pi, \ldots, N\pi\big\}^d.$$

Note that below we will also define a domain that is reciprocal with respect to the unscaled physical space $\mathbb{Z}^d$.

For $u \in \mathscr{U}_N$ we define the Fourier transform $\hat{u} : \widehat{\Omega}_N \to \mathbb{R}^d$ by

$$\hat{u}(k) = \varepsilon^d \sum_{x \in \Omega_N} u(x) \exp(\imath x \cdot k), \tag{1.3}$$

where $\imath$ denotes the imaginary unit. The inversion formula is given by the identity

$$u(x) = \sum_{k \in \widehat{\Omega}_N} \hat{u}(k) \exp(-\imath x \cdot k) \qquad \text{for } x \in \Omega_N. \tag{1.4}$$

The Plancherel theorem for this variant of the Fourier transform reads

$$\varepsilon^d \sum_{x \in \Omega_N} u(x) \cdot v(x) = \sum_{k \in \widehat{\Omega}_N} \hat{u}(k) \cdot \overline{\hat{v}(k)} \qquad \forall u, v \in \mathscr{U}_N.$$

Using (1.3) and (1.4) we can define the trigonometric interpolant $\Pi_N u$ of a lattice function $u \in \mathscr{U}_N$ by

$$\Pi_N u(x) = \sum_{k \in \widehat{\Omega}_N} \hat{u}(k) \exp(-\imath x \cdot k) \qquad \text{for } x \in \Omega. \tag{1.5}$$

When there is no danger of ambiguity we will simply write $u = \Pi_N u$. With this identification we have $u \in \mathrm{C}^\infty_{\mathrm{per}}(\Omega)^d$ with

$$\nabla u(x) = \sum_{k \in \widehat{\Omega}_N} \hat{u}(k) \otimes (-\imath k) \exp(-\imath x \cdot k),$$

and consequently, using the Plancherel theorem,

$$\|\nabla u\|_{\mathrm{L}^2} = \left(\sum_{k \in \widehat{\Omega}_N} |k|^2 |\hat{u}(k)|^2 \right)^{1/2}.$$

1.4.2. *Continuous functions*

The reciprocal domain for continuous functions is simply the "limit" of $\widehat{\Omega}_N$ as $N \to \infty$, that is,

$$\widehat{\Omega} = \pi \mathbb{Z}^d.$$

If $u \in \mathrm{H}^1_{\mathrm{per}}(\Omega)^d$ then its Fourier transform (Fourier series) is defined by

$$\hat{u}(k) = \int_\Omega u(x) \exp(\imath x \cdot k) \, \mathrm{d}x, \qquad \text{for } k \in \widehat{\Omega},$$

and we have the following identities, corresponding to the discrete identities discussed in the previous section (the infinite sums in the first and third lines converge in the strong L^2-topology):

$$\begin{aligned}
u(x) &= \sum_{k \in \widehat{\Omega}} \hat{u}(k) \exp(-\imath x \cdot k), \\
\int_\Omega u \cdot v \, \mathrm{d}x &= \sum_{k \in \widehat{\Omega}} \hat{u}(k) \cdot \overline{\hat{v}(k)}, \\
\nabla u(x) &= \sum_{k \in \widehat{\Omega}} \hat{u}(k) \otimes (-\imath k) \exp(-\imath x \cdot k), \\
\|\nabla u\|_{\mathrm{L}^2} &= \left(\sum_{k \in \widehat{\Omega}} |k|^2 |\hat{u}(k)|^2 \right)^{1/2}.
\end{aligned}$$

We note that it is possible that an ambiguity occurs when we connect continuous and discrete functions as follows. It will be convenient later to interpret a continuous function $u \in \mathrm{C}^0_{\mathrm{per}}(\Omega)^d$ as a discrete function $(u(x))_{x \in \varepsilon \mathbb{Z}^d}$ also. This identification defines an embedding $\mathrm{C}^0_{\mathrm{per}}(\Omega)^d \to \mathscr{U}_N$ and in particular allows us to define $E^N_{\mathrm{a}}(y_{\mathsf{B}} + u)$ for all $u \in \mathrm{C}^0_{\mathrm{per}}(\Omega)^d$. However, in such a situation, $u(x)$ may stand for both the original continuous function and for the trigonometric interpolant of $(u(x))_{x \in \varepsilon \mathbb{Z}^d}$. In the few instances where this occurs we will write $\Pi_N u$ for the trigonometric interpolant.

For future reference we note that

$$\Pi_N u \to u \quad \text{strongly in } \mathrm{C}^{k,\alpha}_{\mathrm{per}}(\Omega) \qquad \text{for all } u \in \mathrm{C}^{k,\alpha}_{\mathrm{per}}(\Omega),$$

for $0 \le k$ and $\alpha \in (0, 1]$; see [13], Theorem 11.6.

1.4.3. *Reciprocal lattices and Brillouin zones*

In our analysis it will often be convenient to rescale the reciprocal domain $\widehat{\Omega}_N$ by $\varepsilon = 1/N$, leading to the sets

$$\widetilde{\Omega}_N = \varepsilon\widehat{\Omega}_N = \big\{\varepsilon\pi(-N+1), \dots, \varepsilon\pi N\big\}^d, \quad \text{and} \quad \widetilde{\Omega} = (-\pi, \pi]^d.$$

We remark that $\widetilde{\Omega}_N$ is the reciprocal domain to the unscaled grid $\{-N+1, \dots, N\}^d$, and that $\widetilde{\Omega}$ is the so-called *first Brillouin zone* for the unscaled infinite lattice $\mathbb{Z}^d$; see [12].

The unscaled lattice $\mathbb{Z}^d$ (or variations thereof) are normally used in the solid state physics literature. Since the present work is focused primarily on the Cauchy–Born continuum limit as $N \to \infty$ we feel that it is more intuitive to define a scaled atomistic domain and energy, which leads to the reciprocal domains $\widehat{\Omega}_N$ and $\widehat{\Omega}$, but revert to working in the Brillouin zone $\widetilde{\Omega}$ through rescaling of certain quantities whenever convenient.

We will normally denote elements of $\widehat{\Omega}$ by k and elements of $\widetilde{\Omega}$ by κ.

2. The Cauchy–Born continuum limit

Recall from Section 1.4.2 that we identify any continuous function $u \in \mathrm{C}^0_{\mathrm{per}}(\Omega)^d$ with the corresponding lattice function $u = (u(x))_{x\in\Omega_N}$, which allows us to define the atomistic energy $E^{\mathrm{a}}_N(y_{\mathsf{B}} + u)$ for any $u \in \mathrm{C}^0_{\mathrm{per}}(\Omega)^d$. With this notation, we obtain the following approximation result. A similar result under different conditions can be found in [2].

Proposition 2.1. *Let $y \in y_{\mathsf{B}} + \mathrm{C}^1_{\mathrm{per}}(\Omega)^d$ such that $\min_\Omega \det(\nabla y) > 0$, then*

$$\lim_{N\to\infty} E^{\mathrm{a}}_N(y) = E^{\mathrm{c}}(y) = \int_\Omega W(\nabla y)\,\mathrm{d}x,$$

where W is the Cauchy–Born stored energy function

$$W(\mathsf{F}) = V(\mathsf{F}\rho; \rho \in \mathscr{R}).$$

Under the stronger smoothness assumption $y \in y_{\mathsf{B}} + \mathrm{C}^3_{\mathrm{per}}(\Omega)^d$, there exists a constant C that may depend on $\|\nabla y\|_{\mathrm{C}^2}$, on $\min_\Omega \det(\nabla y)$ and on $|\nabla^k V|, k = 1, 2$, such that, for all N sufficiently large,

$$\big|E^{\mathrm{a}}_N(y) - E^{\mathrm{c}}(y)\big| \le C\varepsilon^2.$$

For the proof of this result some care needs to be taken in showing that $D_{\mathscr{R}}y(x)$ belongs to D_V. To that end we first establish a more generally useful technical lemma.

Lemma 2.2. *Let $y \in y_{\mathsf{B}} + \mathrm{C}^1_{\mathrm{per}}(\Omega)^d$ such that $\min_\Omega \det \nabla y > 0$, then there exist $\delta > 0$ and $N_* > 0$ such that*

$$D_{\mathscr{R}}y(x) \in D_V^\delta \qquad \forall x \in \Omega_N \quad \forall N \ge N_*.$$

Proof. For each $x \in \Omega$ we define

$$\delta_1(x) := \max\{\delta' > 0 : \nabla y(x)\mathscr{R} \in D_V^{\delta'}\}.$$

Since $\det \nabla y(x) > 0$ it follows that $\delta_1(x) > 0$ for all $x \in \Omega$. Moreover, using the continuity of $\nabla y(x)$, it is easy to see that $\delta_1(x)$ is lower semicontinuous in Ω, and hence the minimum over Ω is attained, that is,

$$\delta_1 := \min_{x\in\Omega} \delta_1(x) > 0.$$

Since $\nabla y - \mathsf{B}$ is continuous and periodic, and hence uniformly continuous, there exists a *modulus of continuity* $\omega : [0, +\infty) \to [0, +\infty)$ such that $\omega(t) \to 0$ as $t \to 0$, and

$$|\nabla y(x) - \nabla y(x')| \leq \omega(|x - x'|).$$

With this notation we have, for each $\rho \in \mathscr{R}$,

$$|D_\rho y(x) - \nabla_\rho y(x)| = \Big| \int_{t=0}^{1} \big[\nabla y(x + t\varepsilon\rho) - \nabla y(x)\big]\rho \, \mathrm{d}t \Big| \leq \omega(\varepsilon|\rho|)|\rho|,$$

which implies

$$\sup_{x \in \Omega_N} \max_{\rho \in \mathscr{R}} |D_\rho y(x) - \nabla_\rho y(x)| \leq \omega\big(\varepsilon \max_{\rho' \in \mathscr{R}} |\rho'|\big)|\rho|.$$

Since we assumed that $\mathscr{R}$ is finite, the right-hand side tends to zero as $\varepsilon \to 0$. From this it follows immediately that $D_{\mathscr{R}} y(x) \in D_V^{\delta_1/2}$ for all $x \in \Omega$ and for ε sufficiently small so that $\max_{\rho \in \mathscr{R}} \omega(\varepsilon|\rho|)|\rho| \leq \frac{1}{2}\delta_1$. □

Proof of Proposition 2.1. Let $y \in y_{\mathsf{B}} + \mathrm{C}^3_{\mathrm{per}}(\Omega)^d$ and, using Lemma 2.2, let $\delta > 0$ (independent of N) and N be sufficiently large so that $D_{\mathscr{R}} y(x) \in D_V^\delta$ for all $x \in \Omega_N$.

We expand $D_\rho y(x)$ to second order,

$$D_\rho y(x) = \nabla_\rho y(x) + \tfrac{1}{2}\varepsilon \nabla_\rho^2 y(x) + O(\varepsilon^2),$$

where, throughout this proof, the terms $O(\varepsilon^2)$ may depend on $\|\nabla y\|_{\mathrm{C}^2}$ and on M_k^δ, $k \leq 2$. Inserting this expansion into V and expanding it also to second order, we obtain

$$V(D_\rho y(x); \rho \in \mathscr{R}) = V(\nabla_\rho y(x); \rho \in \mathscr{R}) + \sum_{\rho \in \mathscr{R}} \partial_\rho V(\nabla_\rho y(x); \rho \in \mathscr{R}) \cdot \left(\frac{1}{2}\varepsilon \nabla_\rho^2 y(x)\right) + O(\varepsilon^2). \tag{2.1}$$

The first-order terms vanish due to the point symmetry of V. To see this, we first note that $\nabla_{-\rho} = -\nabla_\rho$ and, in particular, $\nabla_\rho^2 y(x) = \nabla_{-\rho}^2 y(x)$. Using (1.2), and the fact that $\nabla_\rho y(x) = \nabla y(x)\rho$, we obtain that

$$\partial_\rho V(\nabla_\rho y(x); \rho \in \mathscr{R}) \cdot \left(\frac{1}{2}\varepsilon \nabla_\rho^2 y(x)\right) = -\partial_{-\rho} V(\nabla_\rho y(x); \rho \in \mathscr{R}) \cdot \left(\frac{1}{2}\varepsilon \nabla_{-\rho}^2 y(x)\right),$$

which immediately implies that

$$\sum_{\rho \in \mathscr{R}} \partial_\rho V(\nabla_\rho y(x); \rho \in \mathscr{R}) \cdot \big(\varepsilon \nabla_\rho^2 y(x)\big) = 0. \tag{2.2}$$

Summing (2.1) over $x \in \Omega_N$, and using (2.2), we obtain

$$E_N^{\mathrm{a}}(y) = \varepsilon^d \sum_{x \in \Omega_N} V(\nabla_\rho y(x); \rho \in \mathscr{R}) + O(\varepsilon^2) = \varepsilon^d \sum_{x \in \Omega_N} W(\nabla y(x)) + O(\varepsilon^2).$$

We now observe that the sum on the right-hand side is a midpoint rule quadrature approximation for $E^{\mathrm{c}}(y)$. Since the midpoint rule is exact on piecewise linear functions a straightforward approximation argument yields

$$\big|E_N^{\mathrm{a}}(y) - E^{\mathrm{c}}(y)\big| \leq \varepsilon^2 \|\nabla^2 W(\nabla y)\|_{\mathrm{C}^0} + O(\varepsilon^2),$$

which concludes the proof for the case $y \in y_{\mathsf{B}} + \mathrm{C}^3_{\mathrm{per}}(\Omega)^d$.

The case $y \in y_{\mathsf{B}} + \mathrm{C}^1_{\mathrm{per}}(\Omega)^d$ follows from a straightforward density argument, or, alternatively, by repeating the foregoing proof but using a zeroth order Taylor expansion of $D_\rho y(x)$ instead of a second order expansion. □

Remark 2.3. Under the smoothness assumptions on V made above it follows that $W \in \mathrm{C}^3(D_W)$ where $D_W = \{\mathsf{F} \in \mathbb{R}^{d\times d} : \det \mathsf{F} > 0\}$.

This immediately implies that, if $y \in y_{\mathsf{B}} + \mathrm{C}^1_{\mathrm{per}}(\Omega)^d$ with $\min_\Omega \det \nabla y > 0$, then the map $u \mapsto E^{\mathrm{c}}(y+u)$, $u \in \mathrm{C}^1_{\mathrm{per}}(\Omega)^d$, is three times continuously Fréchet differentiable at 0. Moreover, it is easily seen that $\delta E^{\mathrm{c}}(y)$ is a bounded linear functional on $\mathrm{H}^1_{\mathrm{per}}(\Omega)^d$ and $\delta^2 E^{\mathrm{c}}(y)$ is a bounded linear operator from $\mathrm{H}^1_{\mathrm{per}}(\Omega)^d$ to $[\mathrm{H}^1_{\mathrm{per}}(\Omega)^d]^*$, that is,

$$\delta E^{\mathrm{c}}(y) \in [\mathrm{H}^1_{\mathrm{per}}(\Omega)^d]^* \quad \text{and} \quad \delta^2 E^{\mathrm{c}}(y) \in L(\mathrm{H}^1_{\mathrm{per}}(\Omega)^d, [\mathrm{H}^1_{\mathrm{per}}(\Omega)^d]^*).$$

3. Stability of Bravais lattices

Under the smoothness assumptions made on the interaction potential V it follows that E^{a}_N is twice continuously differentiable at the homogeneous deformation y_{B} (or, the Bravais lattice $\varepsilon\mathsf{B}\mathbb{Z}^d$), provided that $\det \mathsf{B} > 0$. Moreover, it is easy to see that y_{B} is a critical point, that is,

$$\langle \delta E^{\mathrm{a}}_N(y_{\mathsf{B}}), u\rangle = 0 \qquad \forall u \in \mathscr{U}_N,$$

where $\langle\cdot,\cdot\rangle$ is used throughout to denote any duality pairing, in this case between $(\mathscr{U}_N)^*$ and $\mathscr{U}_N$. For some fixed $N \in \mathbb{N}$ we might say that the deformation y_{B} is stable in the atomistic model if

$$\Lambda^N_{\mathrm{a}}(\mathsf{B}) := \inf_{\substack{u\in\mathscr{U}_N \\ \|\nabla u\|_{\mathrm{L}^2}=1}} \langle \delta^2 E^{\mathrm{a}}_N(y_{\mathsf{B}})u, u\rangle \tag{3.1}$$

is positive. However, we are interested in properties that are uniform in N, and hence we use the stronger definition: *the deformation y_{B} (or, the Bravais lattice $\varepsilon\mathsf{B}\mathbb{Z}^d$) is stable in the atomistic model if*

$$\Lambda_{\mathrm{a}}(\mathsf{B}) := \inf_{N\in\mathbb{N}} \Lambda^N_{\mathrm{a}} > 0. \tag{3.2}$$

It is also straightforward to establish that y_{B} is a critical point of the Cauchy–Born functional E^{c}, that is, $\langle \delta E^{\mathrm{c}}(y_{\mathsf{B}}), u\rangle = 0$ for all $u \in \mathrm{H}^1_{\mathrm{per}}(\Omega)^d$, and consequently we define: *the deformation y_{B} is stable in the Cauchy–Born continuum model if*

$$\Lambda_{\mathrm{c}}(\mathsf{B}) := \inf_{\substack{u\in\mathrm{H}^1_{\mathrm{per}}(\Omega)^d \\ \|\nabla u\|_{\mathrm{L}^2}=1}} \langle \delta^2 E^{\mathrm{c}}(y_{\mathsf{B}})u, u\rangle. \tag{3.3}$$

We recall the discussion of differentiability of E^{c} in Remark 2.3, which ensures that the foregoing discussion is meaningful.

For the sake of brevity of the notation we will often write $\Lambda^N_{\mathrm{a}} = \Lambda^N_{\mathrm{a}}(\mathsf{B})$, $\Lambda_{\mathrm{a}} = \Lambda_{\mathrm{a}}(\mathsf{B})$ and $\Lambda_{\mathrm{c}} = \Lambda_{\mathrm{c}}(\mathsf{B})$. Since B is effectively fixed throughout our analysis there is no danger of ambiguity.

Our main result in this section is that stability in the atomistic model implies stability in the continuum model.

Theorem 3.1. *Let $\mathsf{B} \in \mathbb{R}^{d\times d}$ such that $\det \mathsf{B} > 0$, then $\Lambda_{\mathrm{a}}(\mathsf{B}) \le \Lambda_{\mathrm{c}}(\mathsf{B})$.*

The result stated in Theorem 3.1 is a classical result, which can be found in solid state physics text books (see, *e.g.*, [22], p. 89). The first (attempt at a) rigorous proof in the mathematics literature that we are aware of is given in [7], Lemma 3.1. Since, in that proof, the wrong scaling of the reciprocal space was used, which makes a crucial step in the correct argument superfluous, we decided to give a complete rederivation.

The intuition behind this result is that E^{c} is the limit of E^{a}_N for smooth functions (or, long wavelengths). Therefore, we can imagine that to test the stability of E^{c} we always test with smooth perturbations (or, Fourier modes with long wavelengths), whereas E^{a}_N is tested with all possible wavelengths. Mathematically, this is encoded in the observation that $\delta^2 E^{\mathrm{a}}_N \to \delta^2 E^{\mathrm{c}}$ in a pointwise sense that we make precise, and this will immediately lead to a proof of Theorem 3.1 in Section 3.1.

Our second proof, which is given in Section 3.3 largely follows the structure of the proof in [7,22]. We first characterise $\Lambda_{\rm a}$ and $\Lambda_{\rm c}$ in terms of quantities in reciprocal space $\widetilde{\Omega}$, and then compare these quantities to deduce the desired result. We present this (original) proof for two reasons. Firstly, we wanted to point out that the crucial step in the characterisation of $\Lambda_{\rm c}$ is in fact the same observation used in the direct proof, namely, that $\delta^2 E_N^{\rm a} \to \delta^2 E^{\rm c}$ pointwise. Secondly, we require the characterisation of $\Lambda_{\rm a}^N$ and $\Lambda_{\rm a}$ in reciprocal space for our analysis in Sections 4 and 5.

3.1. **Direct proof of Theorem 3.1**

The main observation required for the proof of Theorem 3.1 is that pointwise convergence of the energy implies pointwise convergence of the Hessian functionals.

Lemma 3.2. *Let* $\det \mathsf{B} > 0$ *and let* $u \in {\rm C}^1_{\rm per}(\Omega)^d$ *then*

$$\langle \delta^2 E_N^{\rm a}(y_{\mathsf{B}})u, u\rangle \to \langle \delta^2 E^{\rm c}(y_{\mathsf{B}})u, u\rangle \qquad \textit{as} \quad N \to \infty.$$

Proof. Let $\delta = \frac{1}{2}\max\{\delta' > 0 : (\mathsf{B}\rho)_{\rho\in\mathscr{R}} \in D_V^{\delta'}\}$. Since $\det \mathsf{B} > 0$, it follows that $\delta > 0$. Fix $u \in {\rm C}^1_{\rm per}(\Omega)^d$, then there exists $t_* > 0$ such that

$$D_{\mathscr{R}}(y_{\mathsf{B}} + tu)(x) \in D_V^{\delta} \qquad \forall 0 < t \le t_* \quad \forall x \in \Omega_N \quad \forall N > 0. \tag{3.4}$$

Moreover, without loss of generality, we can choose δ and t_* such that $\det(\mathsf{B} + t\nabla u) \ge \delta$ for all $0 < t \le t_*$. Hence, expanding $E_N^{\rm a}$ and $E^{\rm c}$ to second order gives, for $0 < t \le t_*$,

$$\begin{aligned} E_N^{\rm a}(y_{\mathsf{B}} + tu) &= E_N^{\rm a}(y_{\mathsf{B}}) + \frac{1}{2}t^2\langle \delta^2 E_N^{\rm a}(y_{\mathsf{B}})u, u\rangle + r_N, \quad \text{and} \\ E^{\rm c}(y_{\mathsf{B}} + tu) &= E^{\rm c}(y_{\mathsf{B}}) + \frac{1}{2}t^2\langle \delta^2 E^{\rm c}(y_{\mathsf{B}})u, u\rangle + r, \end{aligned} \tag{3.5}$$

where, for some constant C depending only on M_3^{δ}, but independent of N, t, u,

$$|r| + |r_N| \le Ct^3\|\nabla u\|_{{\rm L}^\infty}^3.$$

Proposition 2.1 implies that $E_N^{\rm a}(y_{\mathsf{B}}) = E^{\rm c}(y_{\mathsf{B}})$, and that

$$E_N^{\rm a}(y_{\mathsf{B}} + tu) \to E^{\rm c}(y_{\mathsf{B}} + tu) \qquad \text{as} \quad N \to \infty.$$

Hence we obtain from (3.5) that

$$\tfrac{1}{2}t^2 \limsup_{N\to\infty} \left|\langle \delta^2 E_N^{\rm a}(y_{\mathsf{B}})u, u\rangle - \langle \delta^2 E^{\rm c}(y_{\mathsf{B}})u, u\rangle\right| \le \limsup_{N\to\infty} |r_N - r| \le Ct^3\|\nabla u\|_{{\rm L}^\infty}^2.$$

Dividing by t^2 and letting $t \to 0$ we obtain the result. □

Proof of Theorem 3.1. Fix $\delta > 0$. Since ${\rm C}^1_{\rm per}(\Omega)^d$ is dense in ${\rm H}^1_{\rm per}(\Omega)^d$, there exists $u_\delta \in {\rm C}^1_{\rm per}(\Omega)^d$ such that $\|\nabla u_\delta\|_{{\rm L}^2} = 1$ and

$$\langle \delta^2 E^{\rm c}(y_{\mathsf{B}})u_\delta, u_\delta\rangle \le \Lambda_{\rm c} + \delta.$$

Thus, according to Lemma 3.2, we also have

$$\lim_{N\to\infty} \langle \delta^2 E_N^{\rm a}(y_{\mathsf{B}})u_\delta, u_\delta\rangle = \langle \delta^2 E^{\rm c}(y_{\mathsf{B}})u_\delta, u_\delta\rangle \le \Lambda_{\rm c} + \delta.$$

Moreover, since $\Pi_N u_\delta \to u_\delta$ strongly in $\mathrm{H}^1_{\mathrm{per}}(\Omega)^d$ it follows that $\|D\Pi_N u_\delta\|_{\mathrm{L}^2} \to \|\nabla u_\delta\|_{\mathrm{L}^2}$, as $N \to \infty$, which implies that

$$\Lambda_{\mathrm{a}} \le \limsup_{N\to\infty} \Lambda_{\mathrm{a}}^N \le \limsup_{N\to\infty} \frac{\langle \delta^2 E_N^{\mathrm{a}}(y_{\mathsf{B}})u_\delta, u_\delta\rangle}{\|D\Pi_N u_\delta\|_{\mathrm{L}^2}^2} = \frac{\langle \delta^2 E^{\mathrm{c}}(y_{\mathsf{B}})u_\delta, u_\delta\rangle}{\|Du_\delta\|_{\mathrm{L}^2}^2} \le \Lambda_{\mathrm{c}} + \delta.$$

Since δ was arbitrary the stated result follows. □

Remark 3.3. It is not too difficult to extend the above proof of Theorem 3.1 to arbitary nonlinear deformations, by showing first, that $\langle \delta E_N^{\mathrm{a}}(y), u\rangle \to \langle \delta E^{\mathrm{c}}(y), u\rangle$ as $N \to \infty$, and second, that $\langle \delta^2 E_N^{\mathrm{a}}(y)u, v\rangle \to \langle \delta^2 E^{\mathrm{c}}(y)u, v\rangle$, for $u, v \in \mathrm{C}^1_{\mathrm{per}}(\Omega)^d$. However, since the remainder of our paper focuses only on homogeneous deformations (and does not extend as easily), we do not present the more general result and the details of the proof here.

3.2. **Fourier transform of the Hessians**

The proof of Theorem 3.1 given in [22] makes heavy use of Fourier analysis. Since the Hessians $\delta^2 E_N^{\mathrm{a}}$ and $\delta^2 E^{\mathrm{c}}$ are evaluated at a homogeneous deformation they are effectively convolution operators and hence the Fourier transform diagonalizes them, which leads to useful explicit characterisations of the stability constants $\Lambda_{\mathrm{a}}^N, \Lambda_{\mathrm{a}}$, and Λ_{c}. In these representations we will construct objects in physical and reciprocal space that are independent of ε, which will require certain rescalings.

After recalling the representation of $\delta^2 E_N^{\mathrm{a}}$ and $\delta^2 E^{\mathrm{c}}$ in reciprocal space, we will review the argument of [22] and show that at its core one uses again Lemma 3.2. Our main reason, however, for reviewing this transformation is that it enables us, in Section 4, to analyze the convergence rate of Λ_{a}^N.

3.2.1. *Fourier transform of* $\delta^2 E_N^{\mathrm{a}}(y_{\mathsf{B}})$

We begin by representing the atomistic Hessian as a convolution operator.

Lemma 3.4. *Let N be sufficiently large so that $\varepsilon\mathscr{R} \subset \Omega_N$, then the Hessian $\delta^2 E_N^{\mathrm{a}}(y_{\mathsf{B}})$ can be written as*

$$\begin{aligned}\langle \delta^2 E_N^{\mathrm{a}}(y_{\mathsf{B}})u, u\rangle &= \varepsilon^{d-2} \sum_{x,x'\in\Omega_N} u(x)^T h\big(\tfrac{x'}{\varepsilon}\big)u(x-x') \\ &= \varepsilon^{d-2} \sum_{x\in\Omega_N} u(x)^T \sum_{\rho\in\mathscr{R}\cup\{0\}} h(\rho)u(x-\varepsilon\rho),\end{aligned} \tag{3.6}$$

where $h : \mathbb{Z}^d \to \mathbb{R}^{d\times d}$ is defined by

$$h(\rho) := \begin{cases} \varepsilon^{-d+2} \frac{\partial^2 E_N^{\mathrm{a}}(y_{\mathsf{B}}+u)}{\partial u(0)\partial u(\varepsilon\rho)}\Big|_{u=0}, & \text{if } \rho \in \mathscr{R}\cup\{0\}, \\ 0, & \text{otherwise.}\end{cases} \tag{3.7}$$

Moreover, h depends only on V, $\mathscr{R}$ and B but is independent of N, and it satisfies the following properties:

$$h(\rho) = h(\rho)^T \qquad \forall \rho \in \mathbb{Z}^d, \tag{3.8}$$

$$h(-\rho) = h(\rho) \qquad \forall \rho \in \mathbb{Z}^d, \qquad \text{and} \tag{3.9}$$

$$h(0) = -\sum_{\rho\in\mathscr{R}} h(\rho). \tag{3.10}$$

Proof. We begin by writing the Hessian $\delta^2 E_N^{\mathrm{a}}(y_{\mathsf{B}})$ in the form

$$\langle \delta^2 E_N^{\mathrm{a}}(y_{\mathsf{B}})u, u\rangle = \sum_{x,x'\in\Omega_N} u(x)^T H(x,x')u(x'),$$

$$\text{where} \qquad H_{ij}(x,x') = \frac{\partial^2 E_N^{\mathrm{a}}(y_{\mathsf{B}}+u)}{\partial u_i(x)\partial u_j(x')}\Big|_{u=0}.$$

We extend the definition of H to take arguments from $\varepsilon\mathbb{Z}^d$ by periodicity:

$$H(x+e_j,x') = H(x,x'+e_i) := H(x,x') \qquad \text{for } x,x' \in \varepsilon\mathbb{Z}^d, \text{ and for } i,j = 1,\dots,d.$$

We also note that, since $E_N^{\rm a}$ is twice continuously differentiable at y_{B},

$$H(x,x') = H(x',x)^T \quad \text{for all } x,x' \in \varepsilon\mathbb{Z}^d. \tag{3.11}$$

For each $u \in \mathscr{U}_N$ and $z \in \varepsilon\mathbb{Z}^d$ define $T_z u(x) = u(x+z)$, then $T_z u \in \mathscr{U}_N$ and it is easy to see that $E_N^{\rm a}(y_{\mathsf{B}} + T_z u) = E_N^{\rm a}(y_{\mathsf{B}} + u)$. This observation immediately implies that

$$\langle \delta^2 E_N^{\rm a}(y_{\mathsf{B}})u, u\rangle = \langle \delta^2 E_N^{\rm a}(y_{\mathsf{B}})T_z u, T_z u\rangle,$$

from which we deduce that

$$H(x,x') = H(x+z,x'+z) \qquad \text{for } x,x',z \in \varepsilon\mathbb{Z}^d, \tag{3.12}$$

and, in particular, that

$$\langle \delta^2 E_N^{\rm a}(y_{\mathsf{B}})u, u\rangle = \sum_{x\in\Omega_N} u(x)^T \sum_{x'\in\Omega_N} H(x-x',0)u(x').$$

Substituting $r = x - x'$ and shifting the summation over r from $x - \Omega_N$ to Ω_N (since all functions are periodic, this does not change the value), we obtain

$$\langle \delta^2 E_N^{\rm a}(y_{\mathsf{B}})u, u\rangle = \sum_{x\in\Omega_N} u(x)^T \sum_{r\in\Omega_N} H(r,0)u(x-r).$$

This form has the advantage that the function $r \mapsto H(r,0)$ only needs to be evaluated in Ω_N. Defining $h(\rho) = \varepsilon^{-d+2}H(\varepsilon\rho,0)$ for $\rho \in \mathscr{R} \cup \{0\}$ and $h(\rho) = 0$ otherwise, which is in fact the definition given in (3.7), concludes the proof of (3.6).

The outer scaling ε^{-d+2} of h and the scaling of its argument was chosen so that h is indeed independent of ε, and takes arguments from $\mathbb{Z}^d$.

To show property (3.9) we choose $z = -x - x'$ in (3.12) to obtain $H(x,x') = H(-x',-x)$. Due to the point symmetry of V, this implies $H(x,x') = H(x',x) = H(-x,-x')$. This immediately gives (3.9).

To show property (3.9) we use the inversion symmetries of V (see (1.1)), which give

$$\begin{aligned} E_N^{\rm a}\big(Fx + u(x)\big) &= E_N^{\rm a}\big(-Fx - u(x)\big), \\ &= E_N^{\rm a}\big(-Fx + u(x)\big), \end{aligned}$$

from which it may be seen that $H(x,x') = H(-x,-x')$.

Property (3.8) follows from the fact that $H(x,x')$ is symmetric for all x,x'. The latter property can be shown by choosing $z = -x - x'$ in (3.12) to obtain $H(x,x') = H(-x',-x)$, and hence, using also (3.11),

$$H_{ij}(x,x') = H_{ji}(x',x) = H_{ji}(-x',-x) = H_{ji}(x,x').$$

Finally, property (3.10) is a consequence of the translation invariance of $E_N^{\rm a}$. Let $u(x) = c \in \mathbb{R}^d$ be a simple translation. Since $E_N^{\rm a}(y_{\mathsf{B}} + tu) = E_N^{\rm a}(y_{\mathsf{B}})$ for all t it follows that

$$0 = \langle \delta^2 E_N^{\rm a}(y_{\mathsf{B}})u, u\rangle = \varepsilon^d \sum_{x\in\Omega_N} \sum_{\rho\in\mathscr{R}\cup\{0\}} c^T h(\rho) c = c^T \left(\sum_{\rho\in\mathscr{R}\cup\{0\}} h(\rho) \right) c.$$

Since this holds for all $c \in \mathbb{R}^d$, and since the matrix in brackets is symmetric, we obtain property (3.10). □

The representation of $\delta^2 E_N^{\rm a}(y_{\mathsf{B}})$ immediately lends itself to a diagonalization *via* the Fourier transform. Some further manipulations of the Fourier transform yield the following lemma. Here, and in our subsequent analysis it will be convenient to use the rescaled reciprocal domains, defined in Section 1.4.3,

$$\widetilde{\Omega}_N = \varepsilon \widehat{\Omega}_N \quad \text{and} \quad \widetilde{\Omega} = (-\pi, \pi]^d.$$

Lemma 3.5. *Let N be sufficiently large so that $\varepsilon\mathscr{R} \subset \Omega_N$, then the Hessian $\delta^2 E_N^{\rm a}(y_{\mathsf{B}})$ can be written as*

$$\langle \delta^2 E_N^{\rm a}(y_{\mathsf{B}})u, u\rangle = \varepsilon^{-2} \sum_{k \in \widehat{\Omega}_N} \hat{u}(k)^T \tilde{h}(\varepsilon k)\overline{\hat{u}(k)},$$

where $\tilde{h} : \widetilde{\Omega} \to \mathbb{R}^{d\times d}$ is defined as

$$\tilde{h}(\kappa) = -\frac{1}{2}\sum_{\rho\in\mathscr{R}} h(\rho) 4\sin^2\left(\frac{1}{2}\kappa\cdot\rho\right).$$

Proof. Fix $u \in \mathscr{U}_N$ then the lattice function $w : \varepsilon\mathbb{Z}^d \to \mathbb{R}^d$ defined by

$$w(x) = \sum_{\rho\in\mathscr{R}\cup\{0\}} h(\rho) u(x - \varepsilon\rho),$$

belongs to $\mathscr{U}_N$. Therefore, (3.6) and Plancherel's theorem imply that

$$\langle \delta^2 E_N^{\rm a}(y_{\mathsf{B}})u, u\rangle = \varepsilon^{-2} \sum_{k \in \widehat{\Omega}_N} \hat{u}(k)\overline{\hat{w}(k)}. \tag{3.13}$$

Noting that w is a convolution we can apply the usual arguments for Fourier transforms of convolutions to show that

$$\hat{w}(k) = \hat{u}(k) \sum_{\rho\in\mathscr{R}\cup\{0\}} h(\rho)\exp\left(\imath\varepsilon k\cdot\rho\right) =: \hat{u}(k)\tilde{h}(\varepsilon k).$$

We use first (3.9) and then (3.10) to rewrite $\tilde{h}$ as follows:

$$\begin{aligned}\tilde{h}(\kappa) &= \sum_{\rho\in\mathscr{R}\cup\{0\}} h(\rho)\exp\left(\imath\kappa\cdot\rho\right) = \frac{1}{2}\sum_{\rho\in\mathscr{R}\cup\{0\}} h(\rho)\big[\exp(\imath\kappa\cdot\rho) + \exp(-\imath\kappa\cdot\rho)\big] \\ &= \frac{1}{2}\sum_{\rho\in\mathscr{R}} h(\rho)\big[\exp(\imath\kappa\cdot\rho) - 1 + \exp(-\imath\kappa\cdot\rho)\big] = -\frac{1}{2}\sum_{\rho\in\mathscr{R}} h(\rho)\, 4\sin^2\left(\tfrac{1}{2}\kappa\cdot\rho\right).\end{aligned}$$

□

3.2.2. *Characterisation of $\Lambda_{\rm a}^N$ and $\Lambda_{\rm a}$*

Using the preparations above we obtain the following result. Here, and throughout, we denote the unit sphere in $\mathbb{R}^d$ by

$$\mathbb{S}^{d-1} = \{a \in \mathbb{R}^d : |a| = 1\}.$$

Theorem 3.6. *Let $\mathsf{B} \in \mathbb{R}^{d\times d}$, $\det \mathsf{B} > 0$, then the following hold:*

(a) *If N is sufficiently large so that $\varepsilon\mathscr{R} \subset \Omega_N$ then the stability constant $\Lambda_{\rm a}^N$ satisfies*

$$\Lambda_{\rm a}^N = \min\left\{v^T\Phi_{\rm a}(\kappa)v : \kappa \in \widetilde{\Omega}_N \setminus \{0\}, v \in \mathbb{S}^{d-1}\right\}, \qquad \textit{where} \tag{3.14}$$

$$\Phi_{\rm a}(\kappa) = \frac{\tilde{h}(\kappa)}{|\kappa|^2} = -\frac{1}{2}\sum_{\rho\in\mathscr{R}} h(\rho)\frac{\sin^2\left(\frac{1}{2}\kappa\cdot\rho\right)}{|\frac{1}{2}\kappa|^2} \quad \textit{for } \kappa \in \widetilde{\Omega}_N \setminus \{0\}.$$

(b) *The uniform stability constant* $\Lambda_{\rm a}$ *satisfies*

$$\Lambda_{\rm a} = \inf\big\{v^T \Phi_{\rm a}(\kappa) v : \kappa \in \widetilde{\Omega} \setminus \{0\}, v \in \mathbb{S}^{d-1}\big\}. \tag{3.15}$$

(c) *In particular,* $\Lambda_{\rm a}^N \to \Lambda_{\rm a}$ *as* $N \to \infty$.

Proof. (a) Let $u \in \mathscr{U}_N$ then, using Lemma 3.5,

$$\begin{aligned}
\langle \delta^2 E_N^{\rm a}(y_{\rm B}) u, u\rangle &= \varepsilon^{-2} \sum_{k \in \widehat{\Omega}_N} \hat{u}(k)^T \tilde{h}(\varepsilon k) \overline{\hat{u}(k)} = \sum_{k \in \widehat{\Omega}_N} |k|^2 \hat{u}(k)^T \frac{\tilde{h}(\varepsilon k)}{|\varepsilon k|^2} \overline{\hat{u}(k)} \\
&\geq \left[\min_{k \in \widehat{\Omega}_N \setminus \{0\}} \min_{\substack{v \in \mathbb{C}^d \\ |v|=1}} v^T \Phi_{\rm a}(\varepsilon k) \overline{v} \right] \sum_{k \in \widehat{\Omega}_N} |k|^2 |\hat{u}(k)|^2 \\
&= \left[\min_{\kappa \in \widetilde{\Omega}_N \setminus \{0\}} \min_{\substack{v \in \mathbb{C}^d \\ |v|=1}} v^T \Phi_{\rm a}(\kappa) \overline{v} \right] \|\nabla u\|_{\rm L^2}^2.
\end{aligned}$$

Since $\Phi_{\rm a}(\kappa)$ is symmetric for all κ, we can replace $v \in \mathbb{C}^d$ by $v \in \mathbb{R}^d$.

To see that this lower bound is attained let $v_* \in \mathbb{R}^d$, and $\kappa_* \in \widetilde{\Omega}_N$ be vectors that attain the minima above. It is then easy to see, setting $k_* = \kappa_*/\varepsilon$, that the function

$$u(x) = -\imath v_* \big[\exp(\imath x \cdot k_*) - \exp(-\imath x \cdot k_*) \big] = 2 v_* \sin(x \cdot k_*),$$

belongs to $\mathscr{U}_N$ and that

$$\frac{\langle \delta^2 E_N^{\rm a}(y_{\rm B}) u, u\rangle}{\|\nabla u\|_{\rm L^2}} = v_*^T \Phi_{\rm a}(\kappa_*) v_*.$$

This concludes the proof of (a).

(b, c) From the characterisation of $\Lambda_{\rm a}^N$ in (*a*) and the definition of $\Lambda_{\rm a}$ it is clear that

$$\Lambda_{\rm a} \geq \inf_{\kappa \in \widetilde{\Omega} \setminus \{0\}} \min_{v \in \mathbb{S}^{d-1}} v^T \Phi_{\rm a}(\kappa) v.$$

Fix $\delta > 0$ then there exists $\kappa \in \widetilde{\Omega} \setminus \{0\}$ and $v \in \mathbb{S}^{d-1}$, such that

$$v^T \Phi_{\rm a}(\kappa) v \leq \inf_{\kappa \in \widetilde{\Omega} \setminus \{0\}} \min_{v \in \mathbb{S}^{d-1}} v^T \Phi_{\rm a}(\kappa) v + \delta.$$

Let $\kappa_N \in \widetilde{\Omega}_N$ be a sequence such that $\kappa_N \to \kappa$ as $N \to \infty$.

From its definition it is obvious that $\tilde{h} \in {\rm C}(\widetilde{\Omega} \setminus \{0\})^{d \times d}$ and hence $\Phi_{\rm a} \in {\rm C}(\widetilde{\Omega} \setminus \{0\})^{d \times d}$. Since

$$v^T \Phi_{\rm a}(\kappa_N) v \to v^T \Phi_{\rm a}(\kappa) v \quad \text{ as } N \to \infty,$$

we obtain that

$$\limsup_{N \to \infty} \Lambda_{\rm a}^N \leq \limsup_{N \to \infty} v^T \Phi_{\rm a}(\kappa_N) v \leq \inf_{\kappa \in \widetilde{\Omega} \setminus \{0\}} \min_{v \in \mathbb{S}^{d-1}} v^T \Phi_{\rm a}(\kappa) v + \delta.$$

Since δ was arbitrary we have

$$\Lambda_{\rm a} \leq \liminf_{N \to \infty} \Lambda_{\rm a}^N \leq \limsup_{N \to \infty} \Lambda_{\rm a}^N \leq \inf_{\kappa \in \widetilde{\Omega} \setminus \{0\}} \min_{v \in \mathbb{S}^{d-1}} v^T \Phi_{\rm a}(\kappa) v \leq \Lambda_{\rm a},$$

which concludes the proof of items (b) and (c). □

3.2.3. *Characterisation of* $\Lambda_{\rm c}$

The classical characterisation of the coercivity constant $\Lambda_{\rm c}$ is the Legendre–Hadamard constant,

$$\Lambda_{\rm c} = \inf_{\kappa,v\in\mathbb{S}^{d-1}} \big(D^2W(\mathsf{B})\big)^d_{i\alpha j\beta=1} v_i v_j \kappa_\alpha \kappa_\beta,$$

which can be found in most texts on systems of elliptic PDE (*e.g.* [10]).

This characterisation of $\Lambda_{\rm c}$ does not lead immediately to an understanding of the relationship between $\Lambda_{\rm c}$ and $\Lambda_{\rm a}$. We will therefore derive a second characterisation directly using the definition of $E^{\rm c}$ as the pointwise limit of $E^{\rm a}_N$ under a globally smooth deformation. In this derivation we essentially replicate an argument in [22], Section 7.

The intuitive idea is that $E^{\rm c}$ is the "long wave-length limit" of $E^{\rm a}_N$, which, in the reciprocal domain $\widetilde{\Omega}$ means that only infinitesimal wave vectors κ are observed. Thus, we will obtain

$$\inf_{\kappa\in\widetilde{\Omega}\setminus\{0\}} \lim_{r\searrow 0} \left[\min_{v\in\mathbb{S}^{d-1}} \frac{\tilde{h}(r\kappa)}{|r\kappa|^2} \right] = \Lambda_{\rm c}. \tag{3.16}$$

Making this argument rigorous and calculating the limit as $r \to 0$ explicitly yields the following result. The result follows essentially from Lemma 3.2, which was also the basis of our direct proof of Theorem 3.1. This is not surprising since a connection between atomistic and continuum Hessians needs to be utilized at some point in the proof of Theorem 3.1, which we will see below is an immediately corollary of (3.16).

Lemma 3.7. *We have the identity*

$$\begin{aligned} \Lambda_{\rm c} = \ & \min\big\{v^T\Phi_{\rm c}(\kappa)v : v,\kappa\in\mathbb{S}^{d-1}\big\}, \\ & \textit{where} \quad \Phi_{\rm c}(\kappa) = -\frac{1}{2}\sum_{\rho\in\mathscr{R}} h(\rho)\frac{(\kappa\cdot\rho)^2}{|\kappa|^2}. \end{aligned} \tag{3.17}$$

Proof. Fix $v\in\mathbb{S}^{d-1}$, and $k\in\widehat{\Omega}\setminus\{0\} = \pi\mathbb{Z}^d\setminus\{0\}$ and define

$$u(x) = v\frac{\sin(k\cdot x)}{|k|^2} = \frac{-2\imath v(\exp(\imath k\cdot x) - \exp(-\imath k\cdot x))}{|k|^2},$$

then $u\in {\rm C}^3_{\rm per}(\Omega)^d$ and $\|\nabla u\|_{{\rm L}^2} = 1$. Using Lemma 3.2 and similar manipulations as in the proof of Theorem 3.6 (a), we obtain

$$\langle \delta^2 E^{\rm c}(y_{\mathsf{B}})u,u\rangle = \lim_{N\to\infty}\langle \delta^2 E^{\rm a}_N(y_{\mathsf{B}})u,u\rangle = \lim_{N\to\infty} v^T\Phi_{\rm a}(\varepsilon k)v.$$

This establishes (3.16), and we are left to compute the limit of $\Phi_{\rm a}(\varepsilon k)$ as $\varepsilon\to 0$.

Invoking the explicit form for $\Phi_{\rm a}$ given in Theorem 3.6,

$$\Phi_{\rm a}(\varepsilon k) = -\frac{1}{2}\sum_{\rho\in\mathscr{R}} h(\rho)\frac{\sin^2(\frac{1}{2}\varepsilon k\cdot\rho)}{|\frac{1}{2}\varepsilon k|^2},$$

and noting that

$$\lim_{\varepsilon\to 0}\frac{\sin^2(\frac{1}{2}\varepsilon k\cdot\rho)}{|\frac{1}{2}\varepsilon k|^2} = \frac{(k\cdot\rho)^2}{|k|^2},$$

we obtain the stated formula. □

3.3. **Proof of Theorem 3.1 in reciprocal space**

As an immediate corollary of (3.16), and of the characterisation of $\Lambda_{\rm a}$ in Theorem 3.6 (b) we obtain a second proof of Theorem 3.1, which is essentially a corrected variant of the proof presented in [7]. Namely, we observe that

$$\Lambda_{\rm a} = \inf_{k\in\widetilde{\Omega}\setminus\{0\}} \left[\min_{v\in\mathbb{S}^{d-1}} \frac{\tilde{h}(\kappa)}{|\kappa|^2} \right] \leq \inf_{\kappa\in\widetilde{\Omega}\setminus\{0\}} \lim_{r\to 0} \left[\min_{v\in\mathbb{S}^{d-1}} \frac{\tilde{h}(r\kappa)}{|r\kappa|^2} \right] = \Lambda_{\rm c}. \tag{3.18}$$

We stress, however, that the crucial ingredient in this proof was again the fundamental property of the Cauchy–Born approximation that

$$\lim_{N\to\infty} \langle \delta^2 E_N^{\rm a}(y_{\mathsf{B}})u, u\rangle = \langle \delta^2 E^{\rm c}(y_{\mathsf{B}})u, u\rangle \qquad \forall u \in {\rm C}^1_{\rm per}(\Omega)^d,$$

which we established in Lemma 3.2, and which was also the main observation for the direct proof presented in Section 3.1.

4. Convergence rates for $\Lambda_{\rm a}^N$

We have seen in Theorem 3.6 that $\Lambda_{\rm a}^N \to \Lambda_{\rm a}$ as $N\to\infty$. The purpose of the present section is to investigate the rate of convergence. The first results of this kind we are aware of can be found in [5], where it is shown in a special case and a slightly different setting that $\Lambda_{\rm a}^N = \Lambda_{\rm a} + O(\varepsilon^2)$. (The analysis in [5] uses piecewise affine instead of trigonometric interpolants to normalize the virtual displacements.) This was used to demonstrate that the Cauchy–Born model, as well as a certain quasicontinuum approximation, can accurately reproduce the critical load for the onset of instability in a 1D tensile experiment.

Questions of this kind are our motivation to investigate this problem in more generality. We understand it as a fundamental theoretical question that can form the basis of more sophisticated results for nonlinear deformations or for atomistic/continuum coupling schemes such as the quasicontinuum method.

Theorem 4.1. *Let* $\mathsf{B}\in\mathbb{R}^{d\times d}$ *with* $\det \mathsf{B} > 0$.

(a) *If* $\Lambda_{\rm a} < \Lambda_{\rm c}$ *then there exists a constant* C *that may depend on* B *and* V *such that*

$$0 \leq \Lambda_{\rm a}^N(\mathsf{B}) - \Lambda_{\rm a}(\mathsf{B}) \leq C\varepsilon^2,$$

(b) *If* $\Lambda_{\rm a} = \Lambda_{\rm c}$ *then there exists a constant* C *that depends only on* $|h(\rho)|$, $\rho\in\mathscr{R}$, *such that*

$$0 \leq \Lambda_{\rm a}^N(\mathsf{B}) - \Lambda_{\rm a}(\mathsf{B}) \leq C\varepsilon.$$

The proof of Theorem 4.1 will be split into two cases, for which different techniques are required. In the first case, covered in Section 4.1, we assume that $\Lambda_{\rm a} < \Lambda_{\rm c}$, which means that the infimum in (3.15) is attained for some κ at some distance from the origin. Since $\Phi_{\rm a}$ is a smooth function in $\widetilde{\Omega}\setminus\{0\}$ we can deduce the result by simply choosing an $O(\varepsilon)$ approximation of κ from $\widetilde{\Omega}_N$.

In the second case, covered in Section 4.2, we assume that $\Lambda_{\rm a} = \Lambda_{\rm c}$, which effectively means that the stability constant $\Lambda_{\rm a}$ is attained for an infinitesimal κ in the representation of Theorem 3.6. Since $\Phi_{\rm a}$ is not smooth near the origin we use the assumption $\Lambda_{\rm a} = \Lambda_{\rm c}$ to construct a sequence $\kappa_N \in \widetilde{\Omega}_N$ that approaches zero at an optimal angle, which is given by the critical wave vector that attains $\Lambda_{\rm c}$.

4.1. **Proof of Theorem 4.1 (a)**

In our first lemma we make precise our earlier statement that if $\Lambda_{\rm a} < \Lambda_{\rm c}$ then the infimum in (3.15) is attained at a point $\bar{\kappa}\in\widetilde{\Omega}\setminus\{0\}$, rephrased as a slightly stronger result.

Lemma 4.2. *The equality* $\Lambda_{\rm a} = \Lambda_{\rm c}$ *holds if and only if*

$$\Lambda_{\rm a} = \inf_{\substack{\kappa\in\widetilde{\Omega}\setminus\{0\}\\ |\kappa|\le\delta}} \min_{v\in\mathbb{S}^{d-1}} v^T\Phi_{\rm a}(\kappa)v \qquad \text{for all } \delta>0, \tag{4.1}$$

where $\Phi_{\rm a}$ *is defined in* (3.14).

In the proof of this lemma we use the following auxilliary result that will also be useful later on.

Lemma 4.3. *Let* $\kappa\in\widetilde{\Omega}\setminus\{0\}$ *and let* $v\in\mathbb{S}^{d-1}$, *then*

$$\left|v^T\Phi_{\rm c}(\kappa)v - v^T\Phi_{\rm a}(\kappa)v\right| \le C|\kappa|^2,$$

where $C = \frac{1}{24}\sum_{\rho\in\mathscr{R}}|\rho|^4|h(\rho)|$.

Proof. A Taylor expansion of $\sin^2(t)$ shows that, for some $\theta\in(0,1)$,

$$t^2 - \sin^2(t) = \frac{1}{3}\cos(2\theta t)t^4 \le \frac{1}{3}t^4.$$

Using this inequality with $t = \frac{1}{2}\kappa\cdot\rho$, and the fact that $|v|=1$, we estimate

$$\begin{aligned}\left|v^T\Phi_{\rm c}(\kappa)v - v^T\Phi_{\rm a}(\kappa)v\right| &= \left|\frac{1}{2}\sum_{\rho\in\mathscr{R}} v^Th(\rho)v\left[\frac{\left(\frac{1}{2}\kappa\cdot\rho\right)^2-\sin^2\left(\frac{1}{2}\kappa\cdot\rho\right)}{\left|\frac{1}{2}\kappa\right|^2}\right]\right|\\ &\le \frac{1}{2}\sum_{\rho\in\mathscr{R}}\left|v^Th(\rho)v\right|\frac{\frac{1}{3}\left(\frac{1}{2}\kappa\cdot\rho\right)^4}{\left|\frac{1}{2}\kappa\right|^2} \le \left[\frac{1}{24}\sum_{\rho\in\mathscr{R}}|\rho|^4\,|h(\rho)|\right]|\kappa|^2.\end{aligned}$$

□

Proof of Lemma 4.2.. Suppose, first, that (4.1) holds. Then there exists a sequence $\kappa_j\in\widetilde{\Omega}\setminus\{0\}$, $\kappa_j\to 0$ as $j\to\infty$, and $v_j\in\mathbb{S}^{d-1}$, such that

$$\Lambda_{\rm a} = \lim_{j\to\infty} v_j^T\Phi_{\rm a}(\kappa_j)v_j.$$

Since the unit sphere in $\mathbb{R}^d$ is compact we may assume, without loss of generality, that $v_j\to\bar v$ as $j\to\infty$. Since $\kappa_j\to 0$ as $j\to\infty$ we obtain from Lemma 4.3 that

$$\Lambda_{\rm c} \le \lim_{j\to\infty} v_j^T\Phi_{\rm c}(\kappa_j)v_j = \lim_{j\to\infty} v_j^T\Phi_{\rm a}(\kappa_j)v_j = \Lambda_{\rm a} \le \Lambda_{\rm c}.$$

This shows that (4.1) implies $\Lambda_{\rm a}=\Lambda_{\rm c}$.

Vice versa, suppose that $\Lambda_{\rm a}=\Lambda_{\rm c}$. Since the unit sphere is compact there exist $\bar\kappa,\bar v\in\mathbb{S}^{d-1}$ such that

$$\Lambda_{\rm c} = \bar v^T\Phi_{\rm c}(\bar\kappa)\bar v.$$

Setting $\kappa_j = \frac{1}{j}\bar\kappa$ and using Lemma 4.3 as well as the fact that $\Phi_{\rm c}(\kappa)$ is homogeneous of degree 0 in κ, we obtain

$$\Lambda_{\rm c} = \Lambda_{\rm a} \le \lim_{j\to\infty}\bar v^T\Phi_{\rm a}(\kappa_j)\bar v = \lim_{j\to\infty}\bar v^T\Phi_{\rm c}(\kappa_j)\bar v = \Lambda_{\rm c}.$$

Hence $\Lambda_{\rm a}=\Lambda_{\rm c}$ implies (4.1). □

As an immediate corollary of Lemma 4.2 we can deduce that, if $\Lambda_{\rm a} < \Lambda_{\rm c}$, then there exist $\bar\kappa \in \widetilde\Omega \setminus \{0\}$ and $\bar v \in \mathbb{S}^{d-1}$, such that

$$\Lambda_{\rm a} = \bar v^T \Phi_{\rm a}(\bar\kappa)\bar v.$$

We now define

$$\varphi_{\rm a}(\kappa) = \bar v^T \Phi_{\rm a}(\kappa)\bar v \qquad \text{for } \kappa \in \widetilde\Omega \setminus \{0\},$$

and we note that $\Lambda_{\rm a} = \varphi_{\rm a}(\bar\kappa)$. From the definition of $\Phi_{\rm a}$ it is clear that $\varphi_{\rm a} \in {\rm C}^\infty(\widetilde\Omega \setminus \{0\})$.

Next, we observe that for each $N \in \mathbb{N}$ there exists a vector $\kappa_N \in \widetilde\Omega_N$ such that

$$|\bar\kappa - \kappa_N| \le \pi\sqrt{d}\,\varepsilon. \tag{4.2}$$

From a Taylor expansion of $\varphi_{\rm a}$ at $\bar\kappa$, noting that $\nabla\varphi_{\rm a}(\bar\kappa) = 0$, we obtain

$$\varphi_{\rm a}(\kappa_N) = \varphi_{\rm a}(\bar\kappa) + \frac{1}{2}(\kappa_N - \bar\kappa)^T \nabla^2\varphi_{\rm a}\big((1-\theta)\bar\kappa + \theta\kappa_N\big)(\kappa_N - \bar\kappa), \tag{4.3}$$

for some $\theta \in (0,1)$. For N sufficiently large so that the segment $\{(1-\theta)\bar\kappa + \theta\bar\kappa_N : \theta \in [0,1]\}$ remains bounded away from the origin, we can use (4.2) and the fact that $\varphi_{\rm a} \in {\rm C}^2(\widetilde\Omega \setminus \{0\})$ to deduce that

$$\big|\varphi_{\rm a}(\kappa_N) - \varphi_{\rm a}(\bar\kappa)\big| \le C\varepsilon^2.$$

In particular, we have

$$0 \le \Lambda_{\rm a}^N - \Lambda_{\rm a} \le \varphi_{\rm a}(\kappa_N) - \varphi_{\rm a}(\bar\kappa) \le C\varepsilon^2,$$

which concludes the proof of Theorem 4.1 in the case $\Lambda_{\rm a} < \Lambda_{\rm c}$.

4.2. **Proof of Theorem 4.1 (b)**

In the second case, $\Lambda_{\rm a} = \Lambda_{\rm c}$, we have to take a different approach. We begin by noting that $\Phi_{\rm a}$ is not even continuous at the origin, which shows that the argument used in the case $\Lambda_{\rm a} < \Lambda_{\rm c}$ is inadequate. Instead we will make direct use of Lemma 4.3.

From the definition of $\Phi_{\rm c}$ in (3.17) and the fact that the unit sphere is compact we see that there exist vectors $\bar\kappa, \bar v \in \mathbb{S}^{d-1}$, such that

$$\Lambda_{\rm c} = \bar v^T \Phi_{\rm c}(\bar\kappa)\bar v.$$

Hence, for any $\kappa_N \in \widetilde\Omega_N$, we have

$$0 \le \Lambda_{\rm a}^N - \Lambda_{\rm a} = \Lambda_{\rm a}^N - \Lambda_{\rm c} \le \bar v^T \Phi_{\rm a}(\kappa_N)\bar v - \bar v^T \Phi_{\rm c}(\bar\kappa)\bar v.$$

We split the difference into two parts,

$$\Lambda_{\rm a}^N - \Lambda_{\rm a} \le \big|\bar v^T \Phi_{\rm a}(\kappa_N)\bar v - \bar v^T \Phi_{\rm c}(\kappa_N)\bar v\big| + \big|\bar v^T \Phi_{\rm c}(\kappa_N)\bar v - \bar v^T \Phi_{\rm c}(\bar\kappa)\bar v\big|, \tag{4.4}$$

which leaves two approximation problems.

The first term on the right-hand side of (4.4) can be estimated, using Lemma 4.3, by

$$\big|\bar v^T \Phi_{\rm a}(\kappa_N)\bar v - \bar v^T \Phi_{\rm c}(\kappa_N)\bar v\big| \le C|\kappa_N|^2. \tag{4.5}$$

To estimate the second term on the right-hand side of (4.4) we first define

$$\varphi_{\rm c}(\kappa) = \bar v^T \Phi_{\rm c}(\kappa)\bar v, \qquad \text{for } \kappa \in \mathbb{S}^{d-1},$$

and note that $\Lambda_c = \varphi_c(\bar\kappa)$. Since $\bar\kappa$ is the minimizer of the constrained minimization problem

$$\min_{\kappa\in\mathbb{S}^{d-1}} \varphi_c(\kappa),$$

and since both φ_c and the compact manifold it is defined on (the unit sphere) are smooth we have

$$|\varphi_c(\kappa) - \varphi_c(\bar\kappa)| \le C|\kappa - \bar\kappa|^2 \qquad \forall \kappa \in \mathbb{S}^{d-1},$$

for some constant C that depends only on $|h(\rho)|, \rho \in \mathscr{R}$. In particular, we obtain

$$\left|\bar v^T \Phi_c(\kappa_N)\bar v - \bar v^T \Phi_c(\bar\kappa)\bar v\right| \le C\left|\frac{\kappa_N}{|\kappa_N|} - \bar\kappa\right|^2. \tag{4.6}$$

Thus, we see that we need to optimize two competing error terms: to make (4.5) small, κ_N should be chosen as small as possible. To make (4.6) small, κ_N should be chosen as large as possible as this facilitates the approximation of $\bar\kappa$ by $\kappa_N/|\kappa_N|$.

The idea is to balance the two competing error terms. We fix some constant $\alpha \in [0,1]$, which we will determine later, and choose $\kappa_N \in \widetilde{\Omega}_N$ such that

$$\left|\kappa_N - \varepsilon^\alpha \bar\kappa\right| \le \sqrt{d}\pi\varepsilon. \tag{4.7}$$

In particular, we have

$$\left||\kappa_N| - \varepsilon^\alpha\right| \le \sqrt{d}\pi\varepsilon,$$

which gives

$$\left|\kappa_N - |\kappa_N|\bar\kappa\right| \le \left|\kappa_N - \varepsilon^\alpha\bar\kappa\right| + \left|(\varepsilon^\alpha - |\kappa_N|)\bar\kappa\right| \le 2\sqrt{d}\pi\varepsilon.$$

Dividing by $|\kappa_N|$ we obtain

$$\left|\frac{\kappa_N}{|\kappa_N|} - \bar\kappa\right| \le C\varepsilon^{1-\alpha}.$$

Combining this result with (4.4), (4.5), and (4.6), we obtain

$$|\Lambda_a^N - \Lambda_a| \le C\left(\varepsilon^{2\alpha} + \varepsilon^{2(1-\alpha)}\right).$$

Choosing $\alpha = 1/2$ balances the two terms on the right-hand side, which gives the optimal asymptotic behaviour and establishes Theorem 4.1 (b).

4.3. **Remarks**

4.3.1. *A sharper variant of Theorem 4.1*

Note that, while the constant in Theorem 4.1 (b) depends only on the magnitude of the coefficients $h(\rho)$, $\rho \in \mathscr{R}$, the constant in Theorem 4.1(a) may also depend on the minimizer $\bar\kappa$. Hence, a finer analysis is desirable.

Recall the Taylor expansion (4.3), from which the constant of the error estimate originates. To obtain a sharper estimate, we use the fact that, by a direct calculation of the second derivative, for any $\kappa \in \widetilde{\Omega} \setminus \{0\}$, we have

$$\left|\nabla^2\varphi_a(\kappa)\right| \le \frac{C_1}{|\kappa|^2},$$

where the constant C_1 depends only on $\sum_{\rho\in\mathscr{R}} |h(\rho)||\rho|^2$. Hence, we obtain that, for sufficiently large N,

$$\Lambda_a^N - \Lambda_a \le C_2\frac{\varepsilon^2}{|\bar\kappa|^2}, \tag{4.8}$$

where C_2 depends only on C_1 and on d. This estimate emphasizes the singular behaviour of $\Phi_{\rm a}$ as $\kappa \to 0$ more clearly.

4.3.2. *Optimality of the convergence rates*

The result in Theorem 4.1 (b) depends crucially on the estimate in (4.7). We wish to show that this estimate is, in some sense, the best possible. To that end we will show that, for certain directions $\bar\kappa$, there is a subsequence $(N_j)_{j=1}^\infty$ and a constant $C > 0$, such that

$$\left|\kappa_{N_j} - \varepsilon^\alpha \bar\kappa\right| \geq C\varepsilon_j \qquad \forall j \in \mathbb{N},$$

where $\varepsilon_j = 1/N_j$. Diving by $\pi\varepsilon_j$, we see that this is equivalent to showing that

$$\left|\pi^{-1}k_{N_j} - \varepsilon_j^{\alpha-1}(\pi^{-1}\bar\kappa)\right| \geq C \qquad \forall j \in \mathbb{N},$$

where $k_N := N\kappa_N \in \widehat{\Omega}_N$, and hence $\pi^{-1}k_{N_j} \in \mathbb{Z}^d$. In view of the equivalence of norms on $\mathbb{R}^d$, we see that this is equivalent to the following statement: *there exists a subsequence $(N_j)_{j=1}^\infty$ and a constant $C > 0$, such that*

$$\min_{p\in\mathbb{Z}} \left|p - N_j^{1-\alpha}x\right| \geq C \qquad \forall j \in \mathbb{N}$$

where $x \in [0, \frac{1}{\pi}]$. To see that this indeed holds, we consider the following results of analytic number theory.

Theorem 4.4 (equidistribution theorem)**.** *Suppose $x \in \mathbb{R}$ is irrational. Define $x_n := nx - \lfloor nx \rfloor$. Then the sequence $(x_n)_{n=1}^\infty$ is uniformly distributed in the unit interval; that is,*

$$\lim_{n\to\infty} \frac{\#(\{x_1, x_2 \ldots, x_n\} \cap [a,b])}{n} = b - a \qquad \textit{for all } a, b \in [0,1].$$

Theorem 4.5 (equidistribution theorem for varying exponent)**.** *Let $x \neq 0$. Then, for all $\alpha \in (0,1)$, the sequence $(x_n)_{n=0}^\infty$ defined by $x_n := n^\alpha x - \lfloor n^\alpha x \rfloor$ is uniformly distributed in the unit interval.*

Both of these results may be found in [17], Exercises 11.1.8, 11.6.3. We note that the results are equivalent to saying that for any subinterval $(a,b) \subseteq [0,1]$, there is a subsequence $(x_{n_j})_{j=1}^\infty$ such that it lies inside that interval for all j. Taking $a = \frac{1}{4}$ and $b = \frac{3}{4}$, and fixing $\alpha \in (0,1]$, we deduce that there is a sequence $(N_j)_{j=1}^\infty$ such that all the terms $xN_j^\alpha - \lfloor xN_j^\alpha \rfloor$ lie in the interval $[\frac{1}{4}, \frac{3}{4}]$. (Note that we do not require x to be irrational in the case where $\alpha = 1$, since, if x is rational and $x < 1$, then there is a subsequence of such terms which appear in this interval an infinite number of times.) For this subsequence, we then have that

$$\left|p_{N_j} - N_j^{1-\alpha}x\right| \geq \frac{1}{4}.$$

We note that the rescaling of $\bar\kappa$ by ε^α only makes sense for $\alpha \leq 1$, and thus we have the result that, generically, the best possible convergence rate is $O(N^{-1})$.

4.3.3. *Remarks on the quadratic rate*

In the previous section we have argued that the convergence rate $O(N^{-1})$ in Theorem 4.1 is optimal. We will now explain why, in some situations, one can nevertheless expect the quadratic rate $O(N^{-2})$ even if $\Lambda_{\rm a} = \Lambda_{\rm c}$.

In one dimension for Lennard–Jones type two-body interaction potentials it was shown in [5] that the convergence rate for $|\Lambda_{\rm a}^N - \Lambda_{\rm a}|$ is always of order $O(\varepsilon^2)$, despite the fact that the weakest eigenmode is always macroscopic, *i.e.*, the case $\Lambda_{\rm a} = \Lambda_{\rm c}$ always holds. The reason for this is that, in one dimension, only one direction in reciprocal space exists and hence the second error term in (4.6) will always vanish. One may therefore

always choose $\kappa_N = O(\varepsilon)$, which leads to the stated convergence rate

$$|\Lambda_{\rm a}^N - \Lambda_{\rm a}| \le C\varepsilon^2, \tag{4.9}$$

for both cases $\Lambda_{\rm a} = \Lambda_{\rm c}$ as well as $\Lambda_{\rm a} < \Lambda_{\rm c}$. We see immediately that this fact remains true for a general interaction potential.

More generally, we observe that (4.9) also remains true whenever the direction κ, which minimises the function

$$\kappa \mapsto \min_{v\in\mathbb{S}^{d-1}} v^T \frac{\Phi_{\rm c}(\kappa)}{|\kappa|^2} v$$

can be reproduced by an $O(\varepsilon)$ vector κ_N. We show that this is the case for the triangular lattice in 2D, but note that, more generally, a similar effect will occur if minimizers lie on high symmetry lines in the Brillouin zone, which is often observed in practice.

The 2D triangular lattice is defined by the transformation matrix

$$\mathsf{B} = \begin{pmatrix} 1 & 1/2 \\ 0 & \sqrt{3}/2 \end{pmatrix}.$$

It is well known that the linearised Cauchy–Born approximation of this configuration is isotropic. In our formulation this is only true in an orthogonal system of coordinates *after* applying B. We therefore define

$$\tilde{W}(\tilde{\mathsf{F}}) := W(\tilde{\mathsf{F}}\mathsf{B}) = W(\mathsf{F}\mathsf{B}^{-1}\mathsf{B})$$

where W is the Cauchy–Born stored energy density $W(\mathsf{F}) = \sum_{\rho\in\mathscr{R}} \phi(|\mathsf{F}\rho|)$. We have the following relation between the elasticity tensors of the two stored energies

$$\tilde{\mathbf{C}}_{i\alpha}^{j\beta} = \mathbf{C}_{i\gamma}^{j\delta}\mathsf{B}_{\alpha\gamma}\mathsf{B}_{\beta\delta}. \tag{4.10}$$

Since $\tilde{W}$ has hexagonal symmetry, it follows that $\tilde{\mathbf{C}}$ is isotropic [14], Section 10, p. 35. From the theory of linearised elasticity [11], Result 7.12, we therefore obtain that

$$\tilde{\mathbf{C}}_{i\alpha}^{j\beta}\mathsf{A}_{i\alpha}\mathsf{A}_{j\beta} = \lambda[\mathrm{tr}(\mathsf{A})]^2 + \tfrac{1}{2}\mu|\mathsf{A}+\mathsf{A}^T|^2,$$

for some Lamé constants $\lambda, \mu \in \mathbb{R}$. Testing $\mathbf{C}$ with $\mathsf{A} = v \otimes k$ and using (4.10) we have

$$\mathbf{C}_{i\alpha}^{j\beta} v_i v_j k_\alpha k_\beta = (\lambda+\mu)(v\cdot\mathsf{B}^{-T}k)^2 + \mu|v|^2|\mathsf{B}^{-T}k|^2 \ge \min(\mu, \lambda+2\mu)|v|^2|\mathsf{B}^{-T}k|^2.$$

This lower bound is attained for, either $v \| k$ or $v \perp k$ depending on the sign of $\lambda+\mu$.

In particular, we see that

$$\min_{v\in\mathbb{S}^{d-1}} \mathbf{C}_{i\alpha}^{j\beta} v_i v_j k_\alpha k_\beta = \min(\mu, \lambda+2\mu)|\mathsf{B}^{-T}k|^2.$$

To obtain the minimum with respect to k we need to compute the smallest eigenvalue of $\mathsf{B}^{-1}\mathsf{B}^{-T}$, which is $2/3$. Hence, it follows that $\Lambda_{\rm c} = \frac{2}{3}\min(\mu, \lambda+2\mu)$. The eigenvector corresponding to the eigenvalue $2/3$ is $k = (0,1)^T$. This "optimal direction" allows us to choose $\kappa_N = (0, \varepsilon\pi)^T$, and we conclude that we obtain again the quadratic convergence rate (4.9), even if $\Lambda_{\rm a} = \Lambda_{\rm c}$.

4.4. Sampling $\widetilde{\Omega}$ with $O(\varepsilon^2)$ convergence rate

Motivated by the linear worst-case convergence rate we obtained in the previous section, we show how to construct grids in $\widetilde{\Omega}$, which can be sampled to obtain an $O(\varepsilon^2)$ convergence rate.

Remark 4.6. To find the lowest eigenvalue it is necessary to obtain a *global* minimiser of $\min_{|v|=1} v^T \Phi_{\rm a}(\kappa) v$ over the Brillouin zone. Locally convergent methods such as descent, Newton, or quasi-Newton methods, are not suitable for this problem.

We take a grid $\mathbb{S}^{d-1}_M$ on the unit sphere with mesh size $\frac{1}{M}$, where $M \in \mathbb{N}$, so that for all $\theta \in \mathbb{S}^{d-1}$,

$$\min_{\theta_M \in \mathbb{S}^{d-1}_M} |\theta - \theta_M| \le \frac{C}{M}.$$

We then use this spherical mesh to create a mesh $\widetilde{\Omega}_M$ over the Brillouin zone by defining

$$\widetilde{\Omega}_M := \left\{ r_M \frac{\theta_M}{|\theta_M|_\infty} : \theta_M \in \mathbb{S}^{d-1}_M, r_M = \frac{\pi}{M}, \frac{2\pi}{M}, \dots, \pi \right\}. \tag{4.11}$$

Such a grid satisfies the following approximation properties.

Lemma 4.7. *Let $\widetilde{\Omega}_M$ be defined by (4.11), then the following statements are true:*

(a) *There exists $C \in \mathbb{R}$ depending only on the dimension, such that for all $\kappa \in \widetilde{\Omega}$, $\min_{\kappa_M \in \widetilde{\Omega}_M} |\kappa - \kappa_M| \le \frac{C}{M}$.*

(b) *There exist constants $C_1, C_2 \in \mathbb{R}$, depending only on the dimension, such that for all $\theta \in \mathbb{S}^{d-1}$, there exists $\kappa_M \in \widetilde{\Omega}_M$ such that $|\kappa_M| \le \frac{C_1}{M}$ and $|\frac{\kappa_M}{|\kappa_M|} - \theta| \le \frac{C_2}{M}$.*

Proof. *(a)* Define $r := |\kappa|$ and $\theta := \frac{\kappa}{|\kappa|}$. Then

$$\begin{aligned}
\left| r\theta - r_M \frac{\theta_M}{|\theta_M|_\infty} \right|^2 &= r^2 - \frac{2 r r_M}{|\theta_M|_\infty} \theta \cdot \theta_M + \frac{r_M^2}{|\theta_M|_\infty^2} \\
&= \left(\frac{r_M}{|\theta_M|_\infty} - r \right)^2 + \frac{r r_M}{|\theta_M|_\infty} (2 - 2\theta \cdot \theta_M) \\
&= \left(\frac{r_M}{|\theta_M|_\infty} - r \right)^2 + \frac{r r_M}{|\theta_M|_\infty} |\theta - \theta_M|^2.
\end{aligned}$$

Now it is clear that we may choose r_M and θ_M such that $|\kappa - \frac{r_M \theta_M}{|r_M|_\infty}| \le \frac{C}{M}$, as $r r_M \le \pi^2$ and $|\theta_M|_\infty \ge \frac{\sqrt{d}}{d}$.

(b) This result follows from the choice of $\mathbb{S}^{d-1}_M$. Pick $r_M = \frac{\pi}{M}$; then, if $\kappa_M := \frac{r_M \theta_M}{|\theta_M|_\infty}$,

$$\left| \frac{\kappa_M}{|\kappa_M|} - \theta \right| = |\theta_M - \theta|,$$

and now a good choice of θ_M gives the result. □

Using the foregoing approximation result, we can now repeat the arguments at the end of Section 4.1 and 4.2 again, but using $\widetilde{\Omega}_M$ instead of $\widetilde{\Omega}_N$. The estimates are essentially the same, but we obtain a better balance due to (b), to obtain the desired $O(M^{-2})$ convergence rate.

Theorem 4.8. *Let $\widetilde{\Omega}_M$ be given by (4.11); then there exists a constant C such that*

$$\min_{\kappa_M \in \widetilde{\Omega}_M} \min_{v \in \mathbb{S}^{d-1}} v^T \Phi_{\rm a}(\kappa_M) v - \Lambda_{\rm a} \le \frac{C}{M^2}. \tag{4.12}$$

5. Equivalence of atomistic and continuum stability

Our analysis in Section 4 shows that computing $\Lambda_{\rm a}(\mathsf{B})$ gives an accurate representation of the stability of the Bravais lattice $\varepsilon\mathsf{B}\mathbb{Z}^d$ for moderately large N. However, $\Lambda_{\rm a}$ is still expensive to compute. In a practical simulation where large nonlinear deformations may occur we would need to test whether $\Lambda_{\rm a}(\mathsf{B}) > 0$ for a large number of deformation gradients B. In [5] it was shown in a special situation (1D, Lennard–Jones type pair interactions) that, in fact, $\Lambda_{\rm a} = \Lambda_{\rm c}$, which considerably simplifies the stability analysis. Such a result would essentially imply, that any stable equilibrium of the Cauchy–Born model corresponds to a stable equilibrium of the atomistic model. The purpose of the present section is to further investigate this interesting question.

In view of the representations of $\Lambda_{\rm a}$ and $\Lambda_{\rm c}$ derived, respectively, in Sections 3.2.2 and 3.2.3, it would be very surprising if such a result would hold in great generality. Indeed, after presenting a simple generalization of the result in [5], we will immediately construct a counterexample. Thus, the question arises whether there are general classes of problems where an equivalence of atomistic and continuum stability may be expected. Our subsequent numerical investigations in this section aim to provide some first examples of this kind.

5.1. **Examples in one dimension**

In one dimension results of this kind have been established for second neighbour Lennard–Jones type pair interactions in [5], which were recently extended to finite range interactions in [16]. We will discuss similar results in the slightly different context of the present paper and also show under which conditions they cease to be valid.

Note that, if the interaction potential V is induced by a pair potential ϕ, that is,

$$V(a_\rho; \rho \in \mathscr{R}) = \sum_{\rho\in\mathscr{R}} \frac{1}{2}\phi(|a_\rho|),$$

then, for $d = 1$,

$$h(\rho) = -\phi''(|\mathsf{B}\rho|), \quad \rho \in \mathscr{R},$$

where h was defined in (3.7). Hence, if the interaction potential has the typical Lennard–Jones type convex-concave shape, then, in realistic deformation regimes, $h(\rho)$ will be negative for $\rho \in \{\pm 1\}$ and positive for $\rho \in \mathscr{R} \setminus \{\pm 1\}$. This motivates the following result.

Proposition 5.1. *Suppose that $d = 1$, that $h(\rho) > 0$ for all $\rho \in \mathscr{R} \setminus \{\pm 1\}$, and that $\Lambda_{\rm c} \geq 0$; then*

$$\Lambda_{\rm a} \geq \frac{4}{\pi^2}\Lambda_{\rm c}.$$

In particular, we have that $\Lambda_{\rm a} > 0$ if and only if $\Lambda_{\rm c} > 0$.

Proof. In one dimension, the characterizations of $\Lambda_{\rm a}$ from (3.15) and $\Lambda_{\rm c}$ from (3.17) can be rewritten in the form

$$\Lambda_{\rm a} = \inf_{\kappa\in(0,\pi]} -\frac{1}{2}\sum_{\rho\in\mathscr{R}} h(\rho)\frac{\sin^2(\frac{1}{2}\kappa\rho)}{(\frac{1}{2}\kappa)^2}, \quad \text{and} \quad \Lambda_{\rm c} = -\frac{1}{2}\sum_{\rho\in\mathscr{R}} h(\rho)\rho^2.$$

Upon defining

$$\psi(t) = \frac{\sin^2(\frac{1}{2}t)}{(\frac{1}{2}t)^2},$$

we may further simplify

$$\Lambda_{\rm a} = \inf_{\kappa\in(0,\pi]} -\frac{1}{2}\sum_{\rho\in\mathscr{R}} h(\rho)\rho^2\psi(\kappa\rho).$$

Next, we show that

$$\psi(\kappa\rho) \le \psi(\kappa) \qquad \forall \kappa \in (0,\pi] \quad \forall \rho \in \mathbb{Z} \setminus \{0\}. \tag{5.1}$$

To see this, we first note that, since $|\sin(t)| \le 1$ we have, for all $t \ge \pi$,

$$\psi(t) \le \frac{1}{(\frac{1}{2}t)^2} \le \frac{1}{(\frac{1}{2}\pi)^2} = \psi(\pi).$$

Second, it can be easily checked that ψ is monotonically decreasing on $(0,\pi]$. Together these two observations imply (5.1).

Using (5.1) we can estimate $\Lambda_{\rm a}$ as follows, recalling that $h(\rho) > 0$ for $\rho \neq \pm 1$:

$$\Lambda_{\rm a} = \inf_{\kappa\in(0,\pi]} -\frac{1}{2}\sum_{\rho\in\mathscr{R}} h(\rho)\rho^2\psi(\kappa\rho) \ge \inf_{\kappa\in(0,\pi]} \left[-\frac{1}{2}\sum_{\rho\in\mathscr{R}} h(\rho)\rho^2\right]\psi(\kappa) = \Lambda_{\rm c} \inf_{\kappa\in(0,\pi]} \psi(\kappa),$$

where, in the last equality, we have used the assumption that $\Lambda_{\rm c} \ge 0$.

Finally, having shown that ψ is monotonically decreasing on $(0,\pi]$ we can compute $\inf_{\kappa\in(0,\pi)} \psi(\kappa) = \psi(\pi) = 4/\pi^2$ to obtain the stated result. □

Conversely, we will now show that, if the hypothesis of Proposition 5.1 is violated, then it is easy to construct an example where $\Lambda_{\rm a} < 0 < \Lambda_{\rm c}$. We note that similar observations for a more realistic EAM potential were made by Li and Luskin [15], Remark 4.4.

To that end suppose that $d = 1$, $\mathscr{R} = \{\pm 1, \pm 2\}$, that $h(\pm 1) = 1$ and $h(\pm 2) = -\frac{1}{2}$. In terms of a two-body interaction potential this would correspond to a potential where $\phi''(\mathsf{B}) = -1$ but $\phi''(2\mathsf{B}) = \frac{1}{2}$. This is unrealistic in the context of Lennard–Jones type models, but such a situation can occur when ϕ has convex regions outside the basin of its minimizer.

Straightforward calculations show that, in this case,

$$\Lambda_{\rm a} = \inf_{\kappa\in(0,\pi)} \frac{2\sin^2(\kappa) - 4\sin^2(\frac{1}{2}\kappa)}{\kappa^2} \le -\frac{4}{\pi^2}, \quad \text{but} \quad \Lambda_{\rm c} = -h(1) - 4h(2) = 1.$$

5.2. **2D triangular lattice with pair interaction**

Motivated by the one-dimensional results of the previous section we study whether atomistic and continuum stability regions also match for lattices in two and three dimensions. It turns out to be difficult to give sharp analytical estimates, hence we present numerical experiments. We refer to appendix 6 for a brief description of our implementation. We begin by discussing the stability of the triangular lattice with Morse potential interaction,

$$\phi(r) = \big[\exp(-2\alpha(r-1)) - 2\exp(-\alpha(r-1))\big]\eta(r), \tag{5.2}$$

where $\eta \in \mathrm{C}^2(\mathbb{R})$ is the unique piecewise quintic cut-off potential chosen so that $\eta(r) = 1$ for $r \le r_1$, and $\eta(r) = 0$ for $r \ge r_2$. Throughout the present section we choose $\alpha = 4$ and $(r_1, r_2) = (3, 5)$.

We parameterise the space of all homogeneous deformations in a neighbourhood of the triangular lattice, which is given by $\mathsf{B} = \mathsf{B}_{\rm tri}$,

$$\mathsf{B}_{\rm tri} = \begin{bmatrix} 1 & 1/2 \\ 0 & \sqrt{3}/2 \end{bmatrix},$$

by three parameters $(v_1, v_2, \theta) \in (0,+\infty)^2 \times (0, 2\pi]$:

$$\mathsf{B}(v_1, v_2, \theta) = \big(v_1 q \otimes q + v_2 q^\perp \otimes q^\perp\big)\mathsf{B}_{\rm tri},$$

where $q = q(\theta) = (\cos(\theta), \sin(\theta))$, and $q^\perp$ is orthogonal to q.

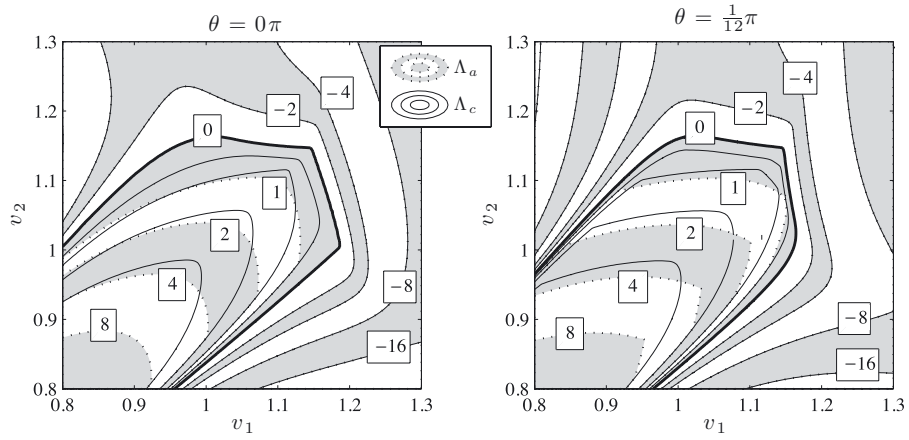

FIGURE 1. Level sets of Λ_a and Λ_c in two-dimensional slices through the space of homogeneous deformations of the 2D triangular lattice, as described in Section 5.2. The levelsets of Λ_a are shaded and drawn in dotted line, while the level sets of Λ_c are drawn in solid lines. Only the levelsets of Λ_a are labelled. We observe that (up to numerical errors) the atomistic and continuum stability regions coincide; and moreover, that all non-positive level sets coincide.

In view of the hexagonal rotational symmetry of the triangular lattice, and reflection symmetry about the plane with normal $(-1/2, \sqrt{3}/2)$, we only need to consider $0 \le \theta \le \pi/12$. In Figure 1 we plot the level lines in the (v_1, v_2) plane of Λ_a and Λ_c, for fixed $\theta \in \{0, \pi/12\}$. We remark that, in view of our asymmetric choice of the Brillouin zone, only the zero level line inherits the symmetry of the deformed lattice, which can be seen in the graph for $\theta = \pi/12$.

We observe in Figure 1 that the zero-level lines for Λ_a and Λ_c indeed coincide (up to numerical errors). Moreover, we observe that in fact all negative level lines coincide as well, which indicates that $\Lambda_a(\mathsf{B}) = \Lambda_c(\mathsf{B})$ whenever $\Lambda_a(\mathsf{B}) < 0$.

We have tested these numerical results by performing more detailed computations in small neighbourhoods of the zero level lines, but did not find any contradictions. However, we stress that it is in principle possible that the discrepancy between the stability regions is simply too small to be easily detected numerically.

We also note that we have obtained analogous results for different parameters of α (we tested $3.5 \le \alpha \le 6$) as well as the Lennard–Jones potential, $\phi(r) = r^{-12} - 2r^{-6}$.

5.3. **The fcc lattice under Lennard–Jones interaction**

In our second set of numerical investigations of stability regions, we explore the fcc lattice with Lennard–Jones interaction,

$$\phi(r) = \left[r^{-12} - 2r^{-6}\right]\eta(r),$$

where η is defined as in the previous section, with parameters $(r_1, r_2) = (4, 6)$. We define the fcc lattice *via* the deformation matrix

$$\mathsf{B}_{\text{fcc}} = \begin{bmatrix} 1 & 1/2 & 1/2 \\ 0 & 1/2 & 0 \\ 0 & 0 & 1/2 \end{bmatrix}.$$

The space of homogeneous deformations (up to rotations) is now six-dimensional, which is far too complex to explore completely. Instead, we only choose two orthonormal matrices (representating orthonormal coordinate

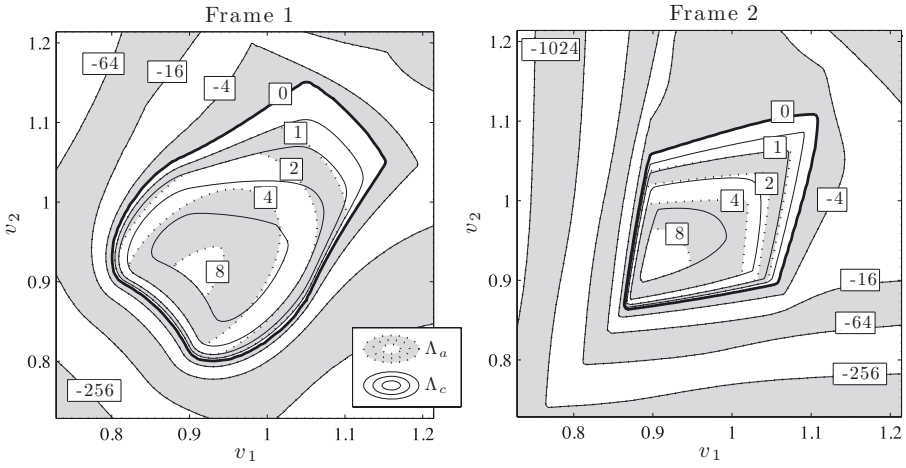

FIGURE 2. Level sets of Λ_a and Λ_c in two-dimensional slices through the space of homogeneous deformations of the fcc lattice, as described in Section 5.3. The bold lines are the zero-level lines. We observe that, up to numerical errors, the atomistic and continuum stability regions coincide.

frames highlighting special symmetry directions in the fcc lattice):

$$\mathsf{Q}_1 = \begin{bmatrix} 1 & 0 & 0 \\ 0 & 1 & 0 \\ 0 & 0 & 1 \end{bmatrix}, \quad \text{and} \quad \mathsf{Q}_2 = \begin{bmatrix} 1/\sqrt{2} & 1/\sqrt{2} & 0 \\ 0 & 0 & 1 \\ -1/\sqrt{2} & 1/\sqrt{2} & 0 \end{bmatrix}.$$

Given these two frames, we test the deformations

$$\mathsf{B}(v_1, v_2, j) = \big(\mathsf{Q}_j \mathrm{diag}(v_1, v_2, v_3)\mathsf{Q}_j^\top\big)\mathsf{B}_\mathrm{fcc},$$

where v_3 is a fixed constant, which is chosen so that the stress-free fcc lattice belongs to the region of deformations that we investigate ($v_3 \approx 0.9712$).

The level lines of the stability constants Λ_a and Λ_c, for fixed j and varying v_1, v_2 are shown in Figure 2. We make the same observations as in the 2D triangular lattice case. If $\Lambda_\mathrm{a} < 0$ then $\Lambda_\mathrm{a} = \Lambda_\mathrm{c}$, which implies that the zero-level lines coincide, and in particular, the atomistic and Cauchy–Born stability regions coincinde as well (up to numerical errors).

5.4. **A counterexample: (in-)stability of bcc**

In our final numerical example, we present a counterexample to our hypothesis of equivalence of atomistic and continuum stability. The example we present was pointed out to us by Ryan Elliott. Following his work in [9], where the stability of a family of complex lattices interacting with a Morse potential is investigated, we begin by investigating (in the Bravais lattice case) for which parameters of α of the Morse potential the BCC lattice is stable. Throughout this section, we fix $(r_1, r_2) = (4, 6)$.

For each α in a region of interest, we first use Newton's method with the matrix

$$\mathsf{B}_\mathrm{bcc} = \frac{2}{\sqrt{3}} \begin{bmatrix} 1 & 0 & 1/2 \\ 0 & 1 & 1/2 \\ 0 & 0 & 1/2 \end{bmatrix}$$

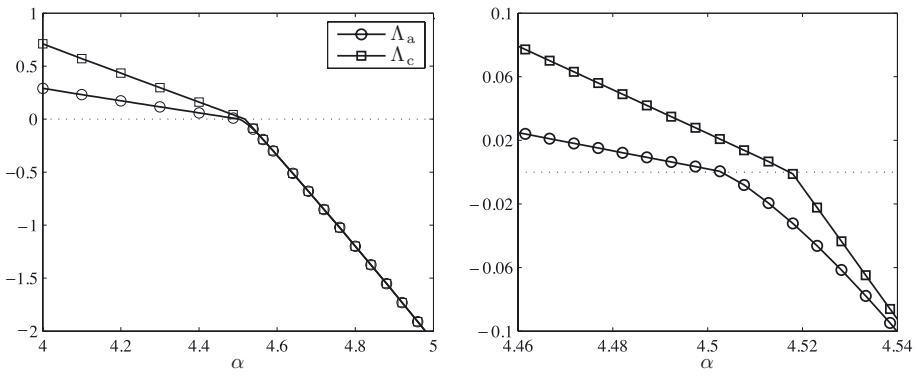

FIGURE 3. Atomistic and Cauchy–Born stability constants in the stress-free bcc crystal under Morse potential interaction for varying stiffness parameter α. The closeup of the region around $\alpha = 4.5$ shows that the Cauchy–Born stability constant remains positive in a wider range of parameters than the atomistic stability constant. The markers in the close-up correspond to the computed datapoints.

as a starting guess to solve the first order optimality condition

$$\frac{\partial W(\mathsf{B})}{\partial \mathsf{B}_{i\alpha}} = 0, \qquad \text{for } i, \alpha = 1, \dots, 3.$$

Upon reorienting the result we obtain a matrix $\mathsf{B}(\alpha)$ of the form $\mathsf{B}(\alpha) = s(\alpha)\mathsf{B}_{\mathrm{bcc}}$, where $s(\alpha)$ is a scalar. The matrix $\mathsf{B}(\alpha)$ (or, $s(\alpha)\mathsf{B}_{\mathrm{bcc}}$) represents the stress-free bcc crystal. We then compute $\Lambda_a(\mathsf{B}(\alpha))$ and $\Lambda_c(\mathsf{B}(\alpha))$ and plot their values against α in Figure 3.

In the first panel, we observe that the stress-free bcc crystal is stable for $\alpha \lesssim 4.5$ but unstable for $\alpha \gtrsim 4.5$. A closeup of the region around $\alpha = 4.5$ shows that Λ_c remains positive for a wider range of parameters than Λ_a.

Remark 5.2. We remark that Figure 3 does *not* imply that there is no stable bcc crystal for $\alpha \gtrsim 4.5$, but only that the stress-free bcc crystal is unstable. As a matter of fact, the bcc configuration is stabilized under uniform compression.

Motivated by the previous numerical experiment, we plot the stability regions for a fixed stiffness parameter $\alpha = 4.45$, in Figure 4. As expected, we observe that the atomistic stability region is strictly contained in the Cauchy–Born stability region.

Remark 5.3. We are unable, at this point, to give a definite explanation of why the stability regions for the 2D triangular lattice and the fcc lattice coincide, but not for the bcc lattice. In view of the counterexample constructed at the end of Section 5.1, it is conveivable, however, that the distance of second neighbours plays a role.

Note that the second neighbour distance in the 2D triangular lattice is $\sqrt{3} \approx 1.73$, and in the fcc lattice it is $\sqrt{2} \approx 1.41$, both of which belong to the concave region of the interaction potential. By contrast, the second neighbour distance in the bcc lattice is only $2/\sqrt{3} \approx 1.15$, which typically still belongs to the convex region of the interaction potential.

6. Conclusion

We have presented a thorough analytical and numerical investigation of the stability of homogeneous Bravais lattices, both in the atomistic description and in the Cauchy–Born description. We have given a new proof of a classical result that atomistic stability implies Cauchy–Born stability, but not vice versa. However, our

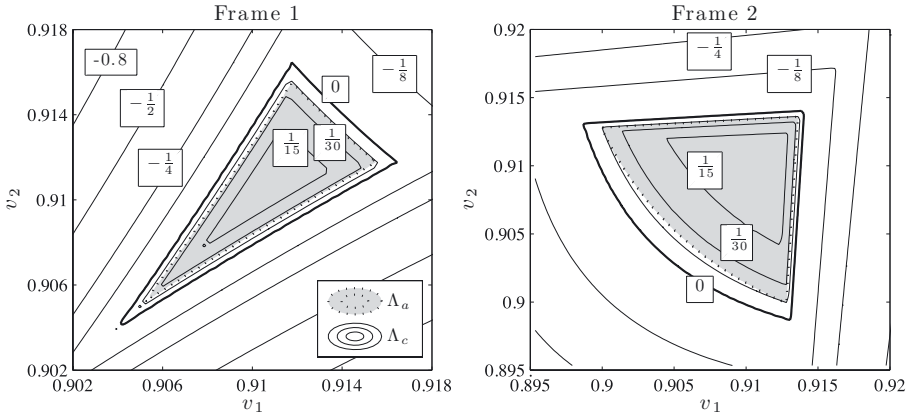

FIGURE 4. The zero level set of Λ_{a} and a selection of level lines of Λ_{c} are plotted in two-dimensional slices through the space of homogeneous deformations of the bcc lattice, as described in Section 5.4. The bold line is the zero-level line of Λ_{c}. We observe that the atomistic stability region (shaded) is strictly contained in the Cauchy–Born stability region.

numerical experiments indicate a general result that the discrepancy between the stability regions should be small or zero in many interesting cases.

In addition to investigating the relationship between atomistic and Cauchy–Born stability regions, we have also analyzed the convergence rate of stability constants in finite lattices to their infinite lattice limits, by estimating the error of sampling the Brillouin zone in a finite subset. Based on our analysis, we have proposed an alternative choice of sampling points with superior convergence rate.

Acknowledgements. We thank Ryan Elliott for pointing out to us the example we presented in Section 5.4, Thomas Bloom for references to the results used in Section 4.3.2, and Mitch Luskin for helpful general discussions.

APPENDIX A. NUMERICAL COMPUTATION OF STABILITY CONSTANTS

In this appendix we give a brief outline of how we compute the stability constants $\Lambda_{\mathrm{c}}, \Lambda_{\mathrm{a}}$ and Λ_{a}^N in our numerical experiments. We stress that our algorithms cannot truly guarantee that global minimizers are found. Only as the initial grid size tends to zero can this be guaranteed. However, we have carefully studied the numerical parameters in our experiments to ensure validity of our numerical results for all practical purposes.

A.1. **Parameterisation of the unit sphere**

We will use two different parameterisations of the unit sphere in 2D and 3D, respectively.

If $d = 2$, we parameterise the unit sphere (*i.e.*, unit circle) by $\theta \in [0, 2\pi)$ and define the corresponding vectors as

$$s(\theta) = (\cos(\theta), \sin(\theta))^\top.$$

If $d = 3$, we parameterise the unit sphere by $(\theta, u) \in [0, \pi) \times [-1, 1]$ and define the corresponding vectors as

$$s(\theta, u) = \left(\sqrt{1-u^2}\cos(\theta), \sqrt{1-u^2}\sin(\theta), u\right)^\top.$$

To obtain a quasi-uniform grid of the unit sphere, we first construct a cartesian grid of the unit cube with $(2M+1)^{d-1}$ gridpoints on each face. These coordinates are then transformed into a quasi-uniform grid $\mathbb{S}_M^{d-1}$ on the unit-sphere *via* rescaling, which also satisfies the conditions of Theorem 4.8.

A.2. **Computation of $\Lambda_{\rm c}$**

We use the characterisation of the stability constant $\Lambda_{\rm c}$ given in (3.17).

(1) We lay a quasi-uniform grid $\mathbb{S}^{d-1}_M$ over the unit sphere in $\mathbb{R}^d$, as described in A.1.
(2) For each $\kappa \in \mathbb{S}^{d-1}_M$ we compute

$$\lambda(\kappa) := \min_{v \in \mathbb{S}^{d-1}} v^\top \Phi_{\rm c}(\kappa) v.$$

(3) We determine $\kappa_0 \in \mathbb{S}^{d-1}_M$ with minimal value $\lambda(\kappa)$, which we pass to a Nelder–Mead simplex algorithm (which operates in parameter space θ or (θ, u)) in order to find a locally optimal value. The output of the Nelder-Mead algorithm is used as the predicted value of $\Lambda_{\rm c}$.

A.3. **Computation of $\Lambda_{\rm a}$**

For the computation of $\Lambda_{\rm a}$ we use the characterisation derived in (3.15). Now, we need to sample not only the unit sphere but the entire Brillouin zone.

(1) We generate the grid $\widetilde{\Omega}_M$ as described in (4.11), where $\mathbb{S}^{d-1}_M$ is constructed as in A.1.
(2) For each $\kappa \in \widetilde{\Omega}_M$ we compute

$$\lambda(\kappa) = \min_{v \in \mathbb{S}^{d-1}} v^\top \Phi_{\rm a}(\kappa) v.$$

(3) We determine the vector κ that minimizes $\lambda(\kappa)$ over the grid $\widetilde{\Omega}_M$ and use it as a starting guess for a Nelder–Mead simplex algorithm. The simplex algorithm operators in the parameter space (r, θ) in 2D, or (r, θ, u) in 3D, which are defined via the coordinate transformations

$$\kappa = \begin{cases} r \frac{s(\theta)}{|s(\theta)|_\infty}, & \text{if } d = 2, \\ r \frac{s(\theta,u)}{|s(\theta,u)|_\infty}, & \text{if } d = 3. \end{cases}$$

The output of the algorithm is used as the predicted value of $\Lambda_{\rm a}$.

To compute $\Lambda^N_{\rm a}$ we simply replace $\widetilde{\Omega}_M$ by the discrete Brillouin zone $\widetilde{\Omega}_N$, and skip the local optimisation step.

Remark A.1. The algorithms we presented in this appendix provide no guarantee that the correct stability constants (*i.e.*, global minimizers) are found. We plan to develop more reliable and more efficient algorithms, based on similar coordinate transformations as those we have construct here in future work.

References

[1] R. Alicandro and M. Cicalese, A general integral representation result for continuum limits of discrete energies with superlinear growth. *SIAM J. Math. Anal.* **36** (2004) 1–37.
[2] X. Blanc, C. Le Bris and P.-L. Lions, From molecular models to continuum mechanics. *Arch. Ration. Mech. Anal.* **164** (2002) 341–381.
[3] M. Born and K. Huang, *Dynamical theory of crystal lattices*. Oxford Classic Texts in the Physical Sciences. The Clarendon Press Oxford University Press, New York, Reprint of the 1954 original (1988).
[4] A. Braides and M.S. Gelli, Continuum limits of discrete systems without convexity hypotheses. *Math. Mech. Solids* **7** (2002) 41–66.
[5] M. Dobson, M. Luskin and C. Ortner, Accuracy of quasicontinuum approximations near instabilities. *J. Mech. Phys. Solids* **58** (2010) 1741–1757.
[6] M. Dobson, M. Luskin and C. Ortner, Sharp stability estimates for the force-based quasicontinuum approximation of homogeneous tensile deformation. *Multiscale Model. Simul.* **8** (2010) 782–802.
[7] W.E and P. Ming, Cauchy–Born rule and the stability of crystalline solids: static problems. *Arch. Ration. Mech. Anal.* **183** (2007) 241–297.

[8] G. Friesecke and F. Theil, Validity and failure of the Cauchy-Born hypothesis in a two-dimensional mass-spring lattice. *J. Nonlinear Sci.* **12** (2002) 445–478.
[9] V.S. Ghutikonda and R.S. Elliott, Stability and elastic properties of the stress-free b2 (cscl-type) crystal for the morse pair potential model. *J. Elasticity* **92** (2008) 151–186.
[10] M. Giaquinta, *Introduction to regularity theory for nonlinear elliptic systems*. Lectures in Mathematics ETH Zürich. Birkhäuser Verlag, Basel (1993).
[11] O. Gonzalez and A.M. Stuart, *A first course in continuum mechanics*. Cambridge Texts in Applied Mathematics. Cambridge University Press, Cambridge (2008).
[12] C. Kittel, *Introduction to Solid State Physics*, 7th ed. John Wiley & Sons, New York, Chichester (1996).
[13] R. Kress, *Linear integral equations*, *Applied Mathematical Sciences* **82**. Springer-Verlag, 2nd edition, New York (1999).
[14] L.D. Landau and E.M. Lifshitz, *Theory of elasticity*, *Course of Theoretical Physics* **7**. Translated by J.B. Sykes and W.H. Reid. Pergamon Press, London (1959).
[15] X.H. Li and M. Luskin, *An analysis of the quasi-nonlocal quasicontinuum approximation of the embedded atom model*. `arXiv:1008.3628v4`.
[16] X.H. Li and M. Luskin, *A generalized quasi-nonlocal atomistic-to-continuum coupling method with finite range interaction.* `arXiv:1007.2336.`
[17] M.R. Murty, *Problems in analytic number theory*, *Graduate Texts in Mathematics* **206**. Springer, 2nd edition, New York (2008). Readings in Mathematics.
[18] C. Ortner, *A priori* and *a posteriori* analysis of the quasinonlocal quasicontinuum method in 1D. *Math. Comput.* **80** (2011) 1265–1285
[19] C. Ortner and E. Süli, Analysis of a quasicontinuum method in one dimension. *ESAIM: M2AN* **42** (2008) 57–91.
[20] B. Schmidt, A derivation of continuum nonlinear plate theory from atomistic models. *Multiscale Model. Simul.* **5** (2006) 664–694.
[21] F. Theil, A proof of crystallization in two dimensions. *Commun. Math. Phys.* **262** (2006) 209–236.
[22] D. Wallace, *Thermodynamics of Crystals*. Dover Publications, New York (1998).
[23] T. Zhu, J. Li, K.J. Van Vliet, S. Ogata, S. Yip and S. Suresh, Predictive modeling of nanoindentation-induced homogeneous dislocation nucleation in copper. *J. Mech. Phys. Solids* **52** (2004) 691–724.